Article

Electrochemical, Spectroscopic, and DFT Study of C(CF) Frontier Orbitals (n = 2–18): The Link between Double Bonds in Pentagons and Reduction Potentials

Alexey A. Popov, Ivan E. Kareev, Natalia B. Shustova, Evgeny B. Stukalin, Sergey F. Lebedkin, Konrad Seppelt, Steven H. Strauss, Olga V. Boltalina, and Lothar Dunsch

J. Am. Chem. Soc., **2007**, 129 (37), 11551-11568• DOI: 10.1021/ja073181e • Publication Date (Web): 24 August 2007

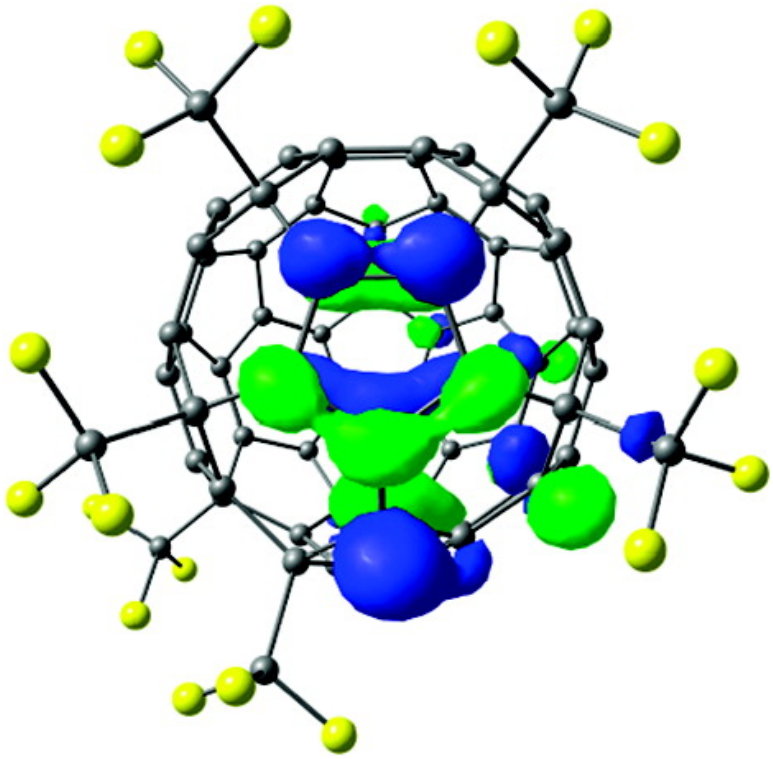

More About This Article

Additional resources and features associated with this article are available within the HTML version:

- Supporting Information
- Links to the 12 articles that cite this article, as of the time of this article download
- Access to high resolution figures

J|A|C|S
ARTICLES
Published on Web 08/24/2007

Electrochemical, Spectroscopic, and DFT Study of $C_{60}(CF_3)_n$ Frontier Orbitals ($n = 2-18$): The Link between Double Bonds in Pentagons and Reduction Potentials

Alexey A. Popov,*[,†,‡] Ivan E. Kareev,[§,||] Natalia B. Shustova,[⊥] Evgeny B. Stukalin,[○] Sergey F. Lebedkin,[||] Konrad Seppelt,[#] Steven H. Strauss,*[,⊥] Olga V. Boltalina,*[,⊥] and Lothar Dunsch*[,‡]

Contribution from the Chemistry Department, Moscow State University, Moscow, 119992, Russia, Department of Electrochemistry and Conducting Polymers, Leibniz Institute for Solid State and Materials Research Dresden, Helmholtzstrasse 20, Dresden D01069, Germany, Institute of Problems of Chemical Physics, Russian Academy of Sciences, Chernogolovka 142432, Russia, Forschungszentrum Karlsruhe, Institute for Nanotechnology, Karlsruhe 76021, Germany, Department of Chemistry, Colorado State University, Fort Collins, Colorado 80523, The James Franck Institute, University of Chicago, Chicago, Illinois 60637, and Institute for Inorganic and Analytical Chemistry, Free University Berlin, D14195 Berlin, Germany

Received May 17, 2007; E-mail: popov@phys.chem.msu.ru; steven.strauss@colostate.edu; ovbolt@lamar.colostate.edu; l.dunsch@ifw-dresden.de

Abstract: The frontier orbitals of 22 isolated and characterized $C_{60}(CF_3)_n$ derivatives, including seven reported here for the first time, have been investigated by electronic spectroscopy ($n = 2$ [1], 4 [1], 6 [2], 8 [5], 10 [6], 12 [3]; the number of isomers for each composition is shown in square brackets) fluorescence spectroscopy ($n = 10$ [4]), cyclic voltammetry under air-free conditions (all compounds with $n \leq 12$), ESR spectroscopy of $C_{60}(CF_3)_n^-$ radical anions at 25 °C ($n = 4$ [1] and 10 [1]), and quantum chemical calculations at the DFT level of theory (all compounds including $n = 16$ [3] and 18 [2]). DFT calculations are also reported for several hypothetical $C_{60}(CF_3)_n$ derivatives. The X-ray structure of one of the compounds, 1,6,-11,16,18,26,36,41,44,57-$C_{60}(CF_3)_{10}$, is reported here for the first time. Most of the compounds with $n \leq 12$ exhibit two or three quasi-reversible reductions at scan rates from 20 mV s^{-1} up to 5.0 V $s^{-1,}$ respectively. The 18 experimental 0/− $E_{1/2}$ values (vs $C_{60}^{0/-}$) are a linear function of the DFT-predicted LUMO energies (average $E_{1/2}$ deviation from the least-squares line is 0.02 V). This linear relationship was used to predict the 0/− $E_{1/2}$ values for the $n = 16$ and 18 derivatives, and none of the predicted values is more positive than the 0/− $E_{1/2}$ value for one of the isomers of $C_{60}(CF_3)_{10}$. In general, reduction potentials for the 0/− couple are shifted anodically relative to the $C_{60}^{0/-}$ couple. However, the 0/− $E_{1/2}$ values for a given composition are strongly dependent on the addition pattern of the CF_3 groups. In addition, LUMO energies for isomers of $C_{60}(X)_n$ ($n = 2$, 4, 6, 8, 10, and 12) that are structurally related to many of the CF_3 derivatives were calculated and compared for X = CH_3, H, Ph, NH_2, CH_2F, CHF_2, F, NO_2, and CN. The experimental and computational results for the $C_{60}(CF_3)_n$ compounds and the computational results for more than 50 additional $C_{60}(X)_n$ compounds provide new insights about the frontier orbitals of $C_{60}(X)_n$ derivatives. For a given substituent, X, the addition pattern is as important, if not more important in many cases, than the number of substituents, n, in determining $E_{1/2}$ values. Those addition patterns with double bonds in pentagons having two C(sp^2) nearest neighbors result in the strongest electron acceptors.

Introduction

The observation that fullerenes and their derivatives are powerful electron acceptors has attracted considerable attention because of the potential applications of these compounds to problems in energy storage and photovoltaic energy conversion.[1−3] The gas-phase electron affinities of C_{60} (≥2.666(1) eV),[4,5] C_{70} (2.676(1) eV),[4] and $C_{76}-D_2(1)$ (2.88(5) eV)[6] rival those of atomic sulfur (2.07 eV) and chlorine (3.61 eV). Multiply charged ions such as C_{60}^{4-} are kinetically stable in the gas phase,[7] and up to six reversible one-electron reductions have been observed in some solvents.[8,9]

† Moscow State University.
‡ Leibniz Institute for Solid State and Materials Research Dresden.
§ Russian Academy of Sciences.
|| Institute for Nanotechnology.
⊥ Colorado State University.
○ University of Chicago.
Free University Berlin.

(1) Nierengarten, J.-F. *New J. Chem.* **2004**, *28*, 1177−1191.
(2) Hoppe, H.; Sariciftci, N. S. *J. Mater. Res.* **2004**, *19*, 1924−1945.
(3) Segura, J. L.; Martin, N.; Guldi, D. M. *Chem. Soc. Rev.* **2005**, *34*, 31−47.
(4) Brink, C.; Andersen, L. H.; Hvelplund, P.; Mathur, D.; Voldstad, J. D. *Chem. Phys. Lett.* **1995**, *233*, 52−54.
(5) Wang, X.-B.; Ding, C.-F.; Wang, L.-S. *J. Chem. Phys.* **1999**, *110*, 8217−8220.
(6) Boltalina, O. V.; Sidorov, L. N.; Borchshevskii, A. Y.; Sukhanova, E. V.; Skokan, E. V. *Rapid Commun. Mass. Spectrom.* **1993**, *7*, 1009−1011.
(7) Cammarata, V.; Guo, T.; Illies, A.; Li, L.; Shevlin, P. *J. Phys. Chem. A* **2005**, *109*, 2765−2767.

The electron-acceptor properties of fullerene$(X)_n$ derivatives, as measured by electrochemical $E_{1/2}$ values, are believed to be modulated primarily by two well-known factors:[10−14] (i) saturation of the fullerene π system (i.e., the value of n), which raises the LUMO energy and makes the first reduction less favorable relative to the parent fullerene; and (ii) the electron-releasing or electron-withdrawing nature of the n substituents, which can augment or diminish the effect of π-system saturation on $E_{1/2}$. One of our goals in fullerene science and technology is to prepare and study a series of fullerene$(X)_n$ derivatives with as wide a range of electron-accepting properties as possible.[15] This will lead to a better understanding of how different X groups, different values of n (for a given X), and different addition patterns (for a given X and a given value of n) affect electrochemical potentials and anion-radical lifetimes (the latter affects the reversibility of the electron-transfer process). Furthermore, a systematic investigation of this type provides detailed information about the nature of the frontier orbitals of fullerene derivatives, and therefore about the reactivity of the derivatives, information that synthetic chemists will be able to use in their pursuit of regioselective addition methodologies.

It is now the case that there are a greater number of isolated and well-characterized homo-addended fullerene$(X)_n$ compounds for $X = CF_3$ than for any other substituent X that forms a 2c−2e$^-$ bond with one cage C atom (for example, there are now 28 fullerene$(CF_3)_n$ X-ray structures and more than 20 additional compounds that have been characterized by other physicochemical methods; see Table S-1 in Supporting Information (SI) for a complete list of references). Among these are 24 $C_{60}(CF_3)_n$ derivatives, which are listed in Table 1.[16−37] (Here and elsewhere, $C_{60}(CF_3)_n$ compounds that have been isolated and characterized will be denoted as **2-1**, **4-1**, etc. The abbreviation for hypothetical $C_{60}(CF_3)_n$ compounds will always carry the suffix **-CF$_3$** for clarity. In addition, abbreviations for $C_{60}(X)_n$ compounds with X other than CF_3, real or hypothetical, will always carry the suffix **-X**.) The addition patterns for 18 of them are shown as Schlegel diagrams in Figure 1. The IUPAC numbering for C_{60} and for 16 of the 18 compounds studied in this work are shown in Figures S-1 and S-2, respectively. Five of the other addition patterns are shown in Figure S-3 (see SI). The compound **18-2-CF$_3$** has not yet been isolated but is also included in Table 1 because it is believed to be the most stable isomer of this composition.[32] The structures of nine of the 18 compounds with $n \leq 12$ are known from X-ray crystallography (**8-1**, **8-2**, **10-2**, **10-3**, **10-4**, **10-5**, **10-6**, **12-1**, **12-2**, and **12-3**), and the structures of four others were elucidated previously by a combination of 1D and 2D ^{19}F NMR spectroscopy and DFT calculations (**2-1**, **4-1**, **6-1**, and **6-2**). Five of the 18 isolated compounds with $n \leq 12$ are reported here for the first time (**8-3**, **8-4**, **8-5**, **10-5**, and **12-3**). Also listed in Table 1 are two addition patterns known from the X-ray structures of $C_{60}(C_2F_5)_6$ and $C_{60}(C_2F_5)_8$ and one addition pattern known from the X-ray structure of $C_{60}(CMe(COOCMe_3)_2)_6$. Schlegel diagrams for these three derivatives are shown in Figure S-4 (see SI).

In this paper we report a combination of electrochemical data, electronic, fluorescence, and ESR spectra, and DFT calculations for the 22 known $C_{60}(CF_3)_n$ derivatives and several hypothetical $C_{60}(CF_3)_n$ derivatives (four of the 0/− $E_{1/2}$ values were briefly reported in 2005[15]). We also report DFT calculations for known or hypothetical $C_{60}(X)_n$ compounds for many of the addition patterns shown in Figure 1 for X = H, Ph, CH_3, CH_2F, CHF_2, NH_2, NO_2, CN. In addition to their fundamental importance, these results suggest strategies for the design of new exohedral fullerene derivatives with an even wider range of electronic properties than is currently available.

(8) Echegoyen, L.; Echegoyen, L. E. *Acc. Chem. Res.* **1998**, *31*, 593−601.
(9) Herranz, M. A.; Echegoyen, L. In *Fullerenes: From Synthesis to Optoelectronic Properties*; Guldi, D. M., Martin, N., Eds.; Kluwer Academic: Dordrecht, The Netherlands, 2002; pp 267−293.
(10) Guldi, D.; Hungerbuhler, H.; Asmus, K. D. *J. Phys. Chem.* **1995**, *99*, 9380−9385.
(11) Boudon, C.; Gisselbrecht, J. P.; Gross, M.; Isaacs, L.; Anderson, H. L.; Faust, R.; Diederich, F. *Helv. Chim. Acta* **1995**, *78*, 1334−1344.
(12) Echegoyen, L.; Diederich, F.; Echegoyen, L. E. In *Fullerenes: Chemistry, Physics, and Technology*; Kadish, K., Ruoff, R., Eds.; Wiley-Interscience: New York, 2000; pp 1−52.
(13) Martin, N.; Sanchez, L.; Illescas, B.; Perez, I. *Chem. Rev.* **1998**, *98*, 2527−2547.
(14) Suzuki, T.; Maruyama, Y.; Akasaka, T.; Ando, W.; Kobayashi, K.; Nagase, S. *J. Am. Chem. Soc.* **1994**, *116*, 1359−1363.
(15) Popov, A. A.; Tarabek, J.; Kareev, I. E.; Lebedkin, S. F.; Strauss, S. H.; Boltalina, O. V.; Dunsch, L. *J. Phys. Chem. A* **2005**, *109*, 9709−9711.
(16) Avent, A. G.; Boltalina, O. V.; Goryunkov, A. V.; Darwish, A. D.; Markov, V. Y.; Taylor, R. *Fullerenes Nanotubes Carbon Nanostruct.* **2002**, *10*, 235−241.
(17) Darwish, A. D.; Abdul-Sada, A. K.; Avent, A. G.; Lyakhovetsky, V. I.; Shilova, E. A.; Taylor, R. *Org. Biomol. Chem.* **2003**, *1*, 3102−3110.
(18) Darwish, A. D.; Avent, A. G.; Abdul-Sada, A. K.; Taylor, R. *Chem. Commun.* **2003**, 1374−1375.
(19) Goryunkov, A. A.; Kuvychko, I. V.; Ioffe, I. N.; Dick, D. L.; Sidorov, L. N.; Strauss, S. H.; Boltalina, O. V. *J. Fluorine Chem.* **2003**, *124*, 61−64.
(20) Goryunkov, A. A.; Ioffe, I. N.; Kuvychko, I. V.; Yankova, T. S.; Markov, V. Y.; Streletskii, A. V.; Dick, D. L.; Sidorov, L. N.; Boltalina, O. V.; Strauss, S. H. *Fullerenes Nanotubes Carbon Nanostruct.* **2004**, *12*, 181−185.
(21) Kareev, I. E.; Shustova, N. B.; Kuvychko, I. V.; Lebedkin, S. F.; Miller, S. M.; Anderson, O. P.; Popov, A. A.; Strauss, S. H.; Boltalina, O. V. *J. Am. Chem. Soc.* **2006**, *128*, 12268−12280.
(22) Kareev, I. E.; Kuvychko, I. V.; Lebedkin, S. F.; Miller, S. M.; Anderson, O. P.; Strauss, S. H.; Boltalina, O. V. *Chem. Commun.* **2006**, 308−310.
(23) Popov, A. A.; Kareev, I. E.; Shustova, N. B.; Peryshkov, D. V.; Miller, S. M.; Anderson, O. P.; Boltalina, O. V.; Strauss, S. H. 2007. Unpublished X-ray structure of **60-12-3** (some disorder; possibly a mixture of two C_2 and one C_{2h} isomers, which have nearly identical DFT-predicted relative energies and DFT-predicted LUMO energies).
(24) Kareev, I. E.; Shustova, N. B.; Newell, B. S.; Miller, S. M.; Anderson, O. P.; Strauss, S. H.; Boltalina, O. V. *Acta Crystallogr.* **2006**, *E62*, o3154−o3156.
(25) Kareev, I. E.; Kuvychko, I. V.; Lebedkin, S. F.; Miller, S. M.; Anderson, O. P.; Seppelt, K.; Strauss, S. H.; Boltalina, O. V. *J. Am. Chem. Soc.* **2005**, *127*, 8362−8375.
(26) Kareev, I. E.; Lebedkin, S. F.; Miller, S. M.; Anderson, O. P.; Strauss, S. H.; Boltalina, O. V. *Acta Crystallogr.* **2006**, *E62*, o1498−o1500. The lowest locants were incorrectly given in this paper as 1,6,11,16,18,26,36,44,48,-58. They should be 1,6,11,16,18,24,27,36,54,60.
(27) Kareev, I. E.; Lebedkin, S. F.; Popov, A. A.; Miller, S. M.; Anderson, O. P.; Strauss, S. H.; Boltalina, O. V. *Acta Crystallogr.* **2006**, *E62*, o1501−o1503.
(28) Kareev, I. E.; Shustova, N. B.; Peryshkov, D. V.; Lebedkin, S. F.; Miller, S. M.; Anderson, O. P.; Popov, A. A.; Boltalina, O. V.; Strauss, S. H. *Chem. Commun.* **2007**, 1650−1652.
(29) Troyanov, S. I.; Dimitrov, A.; Kemnitz, E. *Angew. Chem., Int. Ed.* **2006**, *45*, 1971−1974.
(30) Shustova, N. B.; Kuvychko, I. V.; Bolskar, R. D.; Seppelt, K.; Strauss, S. H.; Popov, A. A.; Boltalina, O. V. *J. Am. Chem. Soc.* **2006**, *128*, 15793−15798.
(31) Dorozhkin, E. I.; Ignat'eva, D. V.; Tamm, N. B.; Vasilyuk, N. V.; Goryunkov, A. A.; Avdoshenko, S. M.; Ioffe, I. N.; Sidorov, L. N.; Pattison, P.; Kemnitz, E.; Troyanov, S. I. *J. Fluorine Chem.* **2006**, *127*, 1344−1348.
(32) Troyanov, S. I.; Goryunkov, A. A.; Dorozhkin, E. I.; Ignat'eva, D. V.; Tamm, N. B.; Avdoshenko, S. M.; Ioffe, I. N.; Markov, V. Y.; Sidorov, L. N.; Scheural, K.; Kemnitz, E. *J. Fluorine Chem.* **2007**, *128*, 545−551.
(33) Canteenwala, T.; Padmawar, P. A.; Chiang, L. Y. *J. Am. Chem. Soc.* **2005**, *127*, 26−27.
(34) Popov, A. A.; Senyavin, V. M.; Troyanov, S. I. *J. Phys. Chem. A* **2006**, *110*, 7414−7421.
(35) Shustova, N. B.; Peryshkov, D. V.; Popov, A. A.; Boltalina, O. V.; Strauss, S. H. *Acta Crystallogr.* **2007**, *E62*, o3129.
(36) Goryunkov, A. A.; Dorozhkin, E. I.; Tamm, N. B.; Ignat'eva, D. V.; Avdoshenko, S. M.; Sidorov, L. N.; Troyanov, S. I. *Mendeleev Commun.* **2007**, *17*, 110−112.
(37) Shustova, N. B.; Peryshkov, D. V.; Kareev, I. E.; Boltalina, O. V.; Strauss, S. H. *Acta Crystallogr.* **2007**, *E63*, o3398.

Table 1. $C_{60}(R_f)_n$ Derivatives (n = 2, 4, 6, 8, 10, 12, 16, 18)[a]

cmpd	addition pattern	abbreviation	synthesis and characterization references: X-ray	^{19}F NMR	DFT
1,7-$C_{60}(CF_3)_2$	C_s-*para* (*p*)	**2-1**		16−19	20, tw
1,6,11,18-$C_{60}(CF_3)_4$	C_1-*pmp*	**4-1**		19	20, tw
1,6,11,18,24,27-$C_{60}(CF_3)_6$	C_1-p^3mp	**6-1**	*b*	19	20, tw
1,6,9,12,15,18-$C_{60}(CF_3)_6$	C_s-SPP[c]	**6-2**		21	21, tw
1,7,16,36,46,49-$C_{60}(C_2F_5)_6$	C_1-*p*,*p*,*p*	**6-3-C_2F_5**	22	22	22, tw
1,23,28,33,38,60-$C_{60}(CF_3)_6$[d]	D_{3d}-(2,6-$C_{10}(CF_3)_2)^6$-loop	**6-4-CF_3**	33[d]		34, tw
1,6,11,16,18,24,27,36-$C_{60}(CF_3)_8$	C_1-p^3mpmp	**8-1**	36,37	tw	tw
1,6,11,18,24,27,52,55-$C_{60}(CF_3)_8$	C_1-p^3mp,*p*	**8-2**	24	tw	tw
1,6,11,18,24,27,53,56-$C_{60}(CF_3)_8$[e]	C_1-p^3mpmp	**8-3**		tw	tw
1,6,11,16,18,28,31,36-$C_{60}(CF_3)_8$[e]	C_1-*pmpmpmp*	**8-4**		tw	tw
1,6,11,18,24,27,33,51-$C_{60}(CF_3)_8$[e,f]	C_1-p^3mp,*p*	**8-5**		tw	tw
1,6,11,18,24,27,32,35-$C_{60}(C_2F_5)_8$	C_1-p^3mp,*p*	**8-6-C_2F_5**	22	22	22, tw
1,6,11,16,18,24,27,36,41,57-$C_{60}(CF_3)_{10}$[e]	C_1-p^3mpmp,*p*	**10-1**		25	tw
1,6,11,16,18,26,36,44,48,58-$C_{60}(CF_3)_{10}$	C_1-$p^3mpmpmp$	**10-2**	26	25	26, tw
1,3,7,10,14,17,23,28,31,40-$C_{60}(CF_3)_{10}$	C_1-*pmp*^{3}*mpmp*	**10-3**	25	25	tw
1,6,12,15,18,23,25,41,45,57-$C_{60}(CF_3)_{10}$	C_2-(p^3m^2-loop)^2	**10-4**	27	tw	27, tw
1,6,11,16,18,26,36,41,44,57-$C_{60}(CF_3)_{10}$	C_1-*pmpmpmpmp*	**10-5**	tw	tw	tw
1,6,11,18,24,27,33,51,54,60-$C_{60}(CF_3)_{12}$	C_1-p^3mpmp,*pmp*	**10-6**	35	tw	tw
1,6,11,16,18,26,36,44,46,49,54,60-$C_{60}(CF_3)_{12}$	S_6-(*pm*)^6-loop	**12-1**	29	30	29,30, tw
1,3,6,11,13,18,26,32,35,41,44,57-$C_{60}(CF_3)_{12}$	C_1-$p^3mpmpmpmp$	**12-2**	28	28	28, tw
1,6,9,12,15,18,43,46,49,52,55,60-$C_{60}(CF_3)_{12}$	$C_{2(h)}$-(2 × SPP)[c]	**12-3**[g]	23	tw	tw
1,3,6,11,13,18,22,28,31,34,37,41,43,46,51,59-$C_{60}(CF_3)_{16}$[h]		**16-1**	32		32, tw
1,3,6,8,11,13,18,23,28,31,34,35,37,50,54,60-$C_{60}(CF_3)_{16}$[h]		**16-2**	32		32, tw
1,3,6,11,13,18,22,24,27,33,41,43,46,49,51,59-$C_{60}(CF_3)_{16}$[h]		**16-3**	32		32, tw
1,3,6,8,11,13,18,23,28,31,34,37,43,46,51,53,56,59-$C_{60}(CF_3)_{18}$[h]		**18-1**	32		32, tw
1,3,6,11,13,18,22,24,27,32,35,37,41,43,46,49,52,54-$C_{60}(CF_3)_{18}$[h]		**18-2-CF_3**			32, tw

[a] tw = this work. [b] This addition pattern has been observed on the C_{60}-like pole of C_{70} in $C_{70}(CF_3)_{10}$. [c] SPP = skew pentagonal-pyramid addition pattern. [d] This is a hypothetical compound based on the X-ray structure of the known compound $C_{60}(CMe(CO_2CMe_3)_6$. [e] This is the most probable addition pattern, but is considered tentative until proven by X-ray crystallography. [f] An equally probable addition pattern differs only in the placement of the isolated hexagon: 1,6,11,18,24,27,51,59-$C_{60}(CF_3)_8$. [g] This product may be a mixture of up to three isomers (two C_2 isomers and one C_{2h} isomer, all with two skew-pentagonal-pyramidal arrays of six CF_3 groups on opposite C_{60} poles. The locants shown here are for the C_{2h} isomer. [h] See Supporting Information for the complex addition patterns of these five derivatives.

Experimental Section

Reagents, Solvents, and Previously Reported $C_{60}(CF_3)_n$ Derivatives. The reagents and solvents CF_3I (Apollo Scientific), C_{60} (Term USA), hexafluorobenzene (Sigma-Aldrich), 1,2-dichlorobenzene (Sigma-Aldrich, 99%, anhydrous), ferrocene ($Fe(Cp)_2$, Fluka), decamethylferrocene ($Fe(Cp^*)_2$, Fluka), cobaltocene ($Co(Cp)_2$, Fluka), chloroform-*d* and benzene-d_6 (Cambridge Isotopes), and heptane and toluene for HPLC purification (Sigma-Aldrich) were used as received. The following solvents and supporting electrolyte for cyclic voltammetry were purified as indicated: dichloromethane (Fluka, puriss. grade; stored in a nitrogen-filled glovebox over 4 Å molecular sieves (Merck)); 1,2-dichlorobenzene (Sigma-Aldrich, ACS grade; distilled from CaH_2 and stored in the glovebox); tetrabutylammonium tetrafluoroborate ($N(n\text{-}Bu)_4BF_4$, Fluka puriss. grade, stored in the glovebox after drying under vacuum at 70 °C for 24 h). The following $C_{60}(CF_3)_n$ derivatives were prepared as previously described: **2-1**, **4-1**, and **6-1**;[19] **6-2**;[21] **8-2**;[24] **10-1**, **10-2**, and **10-3**;[25] **10-4**;[27] **12-1**;[28,29] and **12-2**.[28]

Synthesis and Isolation of 8-1, 8-3, 8-4, 8-5, 10-5, 10-6, and 12-3. In a typical experiment, finely ground C_{60} (150 mg, 0.208 mmol) was placed in a 0.8-cm I.D. glass tube connected to a gas handling system at one end and a mineral-oil bubbler at the other. The portion of the tube containing C_{60} was placed in a 5-cm long tube furnace. After purging the sample with argon, it was heated to 460 °C and treated with 12 sccm of gaseous CF_3I (ca. 0.05 mmol min^{-1}) for 2 h [CAUTION: CF_3I decomposes in air above 300 °C and produces toxic HF, COF_2, and I_2; handle only in a well-ventilated fume hood]. Orange-brown $C_{60}(CF_3)_n$ derivatives and purple I_2 condensed inside the tube approximately 1 cm outside of both ends of the furnace (i.e., in the cold zones). Iodine was removed under a flow of argon with mild heating (≤100 °C).

The orange-brown condensate (a total of 600 mg from several preps) was purified by HPLC as follows. In the first stage of purification (20-mm I.D. × 250 mm Cosmosil Buckyprep column, Nacalai Tesque, Inc.; 300 nm UV detector; 18 mL min^{-1} eluent flow rate), 1.8-mL injections were eluted with toluene to give eight fractions. In the second stage, 1.8 mL-injections of each fraction were eluted with 20/80 (v/v) toluene/hexane. One first-stage fraction contained several isomers of $C_{60}(CF_3)_{12}$, one of which (**60-12-3**) was isolated to 98+% purity using 100% heptane as eluent (its retention time on a 10-mm I.D. × 250 mm Buckyprep column was 5.9 min at 3 mL/min flow rate). One second-stage fraction contained primarily two isomers, **10-1** and **10-2**, which were separated as narrow cuts and isolated by solvent evaporation (80+ mol % purity). They were further purified to 90% and 98%, respectively, by a third HPLC stage using 100% heptane (10-mm I.D. × 250 mm Cosmosil Buckyprep column, Nacalai Tesque, Inc.; 300-nm UV detector; 5 mL min^{-1} flow rate, retention times 10.4 min for **10-1** and 14.7 min for **10-2**). Another second-stage fraction contained primarily **10-3** and smaller amounts of **10-4** and **10-5**. A third stage of HPLC purification of this fraction (same conditions as second stage) using 20/80 toluene/hexane consisted of collecting a cut from 15.2 to 16.8 min. This contained **10-3** with 95+% purity. The compounds **10-4** and **10-5** had 20/80 toluene/hexane retention times of 11.2 and 7.3 min, respectively, and were also isolated with 95+% purity. Compound **60-10-6** (95+% purity) was isolated from a 500 °C hot-tube reaction product using a 10-mm I.D. × 250 mm Buckyprep column. Its retention time in 100% heptane at 3 mL/min flow rate was 21 min.

The five isomers of $C_{60}(CF_3)_8$ were isolated from the 4.5−6.5 min first-stage fraction. Second-stage purification using 20/80 toluene/heptane resulted in the collection of **8-1**, **8-2**, **8-3**, **8-4**, and **8-5** at 13.5, 14.5, 16.0, 18.8, and 19 min, respectively. Two more stages of HPLC

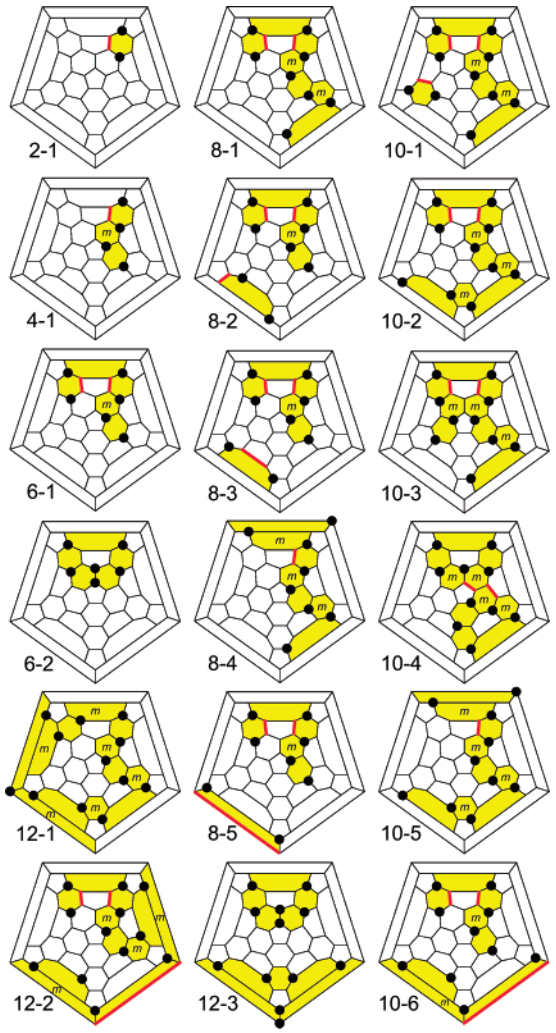

Figure 1. Schlegel diagrams for the 18 $C_{60}(CF_3)_n$ compounds investigated with $n \leq 12$. The black circles indicate the cage carbon atoms to which the CF_3 groups are attached. The isolated *p*-$C_6(CF_3)_2$ hexagons and the ribbons and loops of edge-sharing *m*- and *p*-$C_6(CF_3)_2$ hexagons are highlighted, and the *m*-$C_6(CF_3)_2$ hexagons are indicated with the letter *m*. The diagrams have been drawn to show similarities in parts of their addition patterns, not to depict the lowest locants relative to a fixed numbering scheme. IUPAC lowest-locant Schlegel diagrams for all but two of the compounds investigated are shown in the Supporting Information. The bonds highlighted in red are those double bonds in pentagons that have two C(sp^2) nearest neighbors.

purification under the same conditions resulted in 90+% pure samples of these compounds except for **8-2**, which was contaminated with ca. 40% of **8-3** (confirmed by ^{19}F NMR spectroscopy; see Figure S-5 in SI).

Physicochemical Measurements. Cyclic voltammetry experiments were carried out in the glovebox (water and oxygen content below 1 ppm) in a one-compartment electrochemical cell. The electrolyte solution was 0.1 M N(*n*-Bu)$_4BF_4$ in dichloromethane except for **12-1**, which for solubility reasons was 0.1 M N(*n*-Bu)$_4BF_4$ in 1,2-dichlorobenzene. Control experiments with several $n < 12$ derivatives demonstrated that the potentials in both solvents relative to C_{60} potentials were within ± 0.01 V, which is the same as the experimental error in measured potentials. The working electrode was a platinum wire terminated with a platinum plate (0.04 cm^2) for $n < 12$ except for **10-6** and was a glassy-carbon electrode for **10-6**, **12-1**, **12-2**, and **12-3**. For all compounds, a platinum wire loop and a silver wire served as the counter electrode and quasi-reference electrode, respectively. The potentials were measured relative to the $Fe(Cp^*)_2^{+/0}$ or $Fe(Cp)_2^{+/0}$ potentials (i.e., either $Fe(Cp^*)_2$ or $Fe(Cp)_2$ was added as an internal standard). The experiments were controlled by a PAR 263 or 273A potentiostat/galvanostat. The ESR spectrum of the radical anion **4-1**$^-$ was recorded using a spectroelectrochemical cell with a laminated platinum-mesh working electrode (1024 meshes/cm^2; 0.08 cm^2 active surface area; silver wire quasi-reference electrode (see above)). The airtight cell was filled with a dichloromethane solution of **4-1** and 0.1 M N(*n*-Bu)$_4BF_4$ in the glove box and transferred to the Bruker ER4104OR optical cavity of a Bruker X-band EPR spectrometer. The potential was held at −0.1 V vs $C_{60}^{0/-}$ and the ESR spectrum was recorded. The ESR spectrum of the **10-2**$^-$ radical anion was recorded with the same instrumentation. The sample was a 1,2-dichloromethane solution of **10-2** to which 1 equiv of $Co(Cp)_2$ had been added. Electronic spectra of dichloromethane and/or toluene solutions of the $C_{60}(CF_3)_n$ compounds were recorded using a Shimadzu 3100 or a Varian Cary 500 spectrophotometer. Emission spectra of toluene solutions were recorded using a Spex Fluorolog-3 spectrometer. The emission was detected in a 90° geometry using a Hamamatsu R928 photomultiplier sensitive in the visible region to ca. 850 nm. Emission spectra were corrected for the wavelength-dependent instrument response. Fluorine-19 NMR spectra of chloroform-*d* or benzene-d_6 solutions containing a small amount of hexafluorobenzene as an internal standard (δ −164.9) were recorded at 25 °C using a Varian INOVA-unity 400 spectrometer operating at 367.45 MHz.

DFT Calculations. Geometry optimization of all structures in both neutral and anionic forms was done in vacuo with the use of the PBE functional[38] and the TZ2P-quality basis set implemented in PRIRODA package.[39] Evaluation of Coulombic and exchange-correlation terms was accelerated by expansion of the electron density in an auxiliary basis set.[39] The molecular geometry optimization using this methodology typically took two or 3 days with one Opteron CPU (in contrast, molecular geometry optimization with hybrid functionals such as B3LYP typically takes weeks).

Single-point energy calculations at the B3LYP/6-311G* level in vacuo and in dichloromethane were carried out using the Gaussian 03 package (these calculations typically took several days for each $C_{60}(CF_3)_n$ molecule or $C_{60}(CF_3)_n^{m-}$ ion with one Opteron CPU).[40] Electrostatic contributions to the solvation energy were evaluated using the conductor-like polarizable continuum model (C-PCM)[41,42] as implemented in Gaussian 03. To construct the cavity encapsulating the solute, we used PBE0/6-31G*-optimized atomic radii (UAKS method in Gaussian 03) because they provide the most balanced description for both neutral and charged solutes when coupled to DFT computations.[43] To avoid artificial solvation inside the fullerene cage, an additional sphere with radius 3.5 Å placed at the center of C_{60} was added to the cavity.

X-ray Diffraction. Crystals of **10-5** were grown by slow evaporation from a saturated *p*-xylene solution at 23 °C. X-ray diffraction data were recorded on a Bruker Smart CCD 1000 TU diffractometer employing Mo K_α radiation (graphite monochromator), a scan width of 0.3° in ω, and a measuring time of 40 s/frame, obtaining a full shell of 1800 frames up to $2\theta = 54.0°$. Selected details related to this crystallographic experiment are listed in Table 2.

The structure was solved by using direct methods and refined (on F^2, using all data) by a full-matrix, weighted least-squares process. Absorption and other corrections were applied by using SADABS.[44] All non-hydrogen atoms were refined by using anisotropic displacement parameters. Hydrogen atoms were placed in idealized positions and

(38) Perdew, J. P.; Burke, K.; Ernzerhof, M. *Phys. Rev. Lett.* **1996**, *77*, 3865−3868.
(39) Laikov, D. N. *Chem. Phys. Lett.* **1997**, *281*, 151−156.
(40) Frisch, M. J.; et al. *Gaussian 03*, revision C.02; Gaussian, Inc.: Wallingford, CT, 2004.
(41) Barone, V.; Cossi, M. *J. Phys. Chem. A* **1998**, *102*, 1995−2001.
(42) Cossi, M.; Rega, N.; Scalmani, G.; Barone, V. *J. Comput. Chem.* **2003**, *24*, 669−681.
(43) Takano, Y.; Houk, K. N. *J. Chem. Theory Comput.* **2005**, *1*, 70−77.
(44) Sheldrick, G. M. *SADABS*: A program for area detector absorption corrections. Bruker AXS Inc.: Madison, 2003.

Table 2. Crystal Data and Structure Refinements for C_1-*pmpmpmpmp*-$C_{60}(CF_3)_{10}$ (**10-5**)

cmpd	1,6,11,16,18,26,36,41,44,57-$C_{60}(CF_3)_{10}$·*p*-$C_6H_4(CH_3)_2$
molecular formula	$C_{78}H_{10}F_{30}$
formula weight	1516.86 g mol^{-1}
crystal system, space group, *Z*	triclinic, $P\bar{1}$, 2
color of crystal	orange
unit cell dimensions	
a (Å)	12.310(3)
b (Å)	14.197(3)
c (Å)	16.002(3)
α (deg)	90.100(5)
β (deg)	107.630(5)
γ (deg)	98.136(5)
temperature (K)	173(2)
final *R* indices[a] [$I > 2\sigma(I)$]	$R_1 = 0.0507$, $wR_2 = 0.1129$
goodness-of-fit on F^2	1.010

[a] $R_1 = (\sum||F_o| - |F_c||)/\sum|F_o|$; $wR_2 = (\sum[w(F_o^2 - F_c^2)^2]/\sum[w(F_o^2)^2])^{1/2}$.

refined by using a riding model. Bruker APEX2 software was employed for data collection and reduction, and Bruker SHELXTL[45] software was used for structure solution, refinement, and graphics.

Results

NMR Spectroscopy. Fluorine-19 NMR spectra of **8-1**, **8-2**, **8-3**, **8-4**, **8-5**, **10-4**, **10-5**, **10-6**, and **12-3** are reported here for the first time and are shown in Figure S-5 (see SI). The purity of these nine derivatives is greater than 90% except for the sample of **8-2**, which also contained ca. 40% of **8-3**, and the sample of **8-5**, which contained ca. 20% of an unidentified isomer of $C_{60}(CF_3)_8$. All nine spectra consist of the appropriate number of multiplets that are either quartets, quartets of quartets, or (in the sole case of **12-3**) quartets of quartets of quartets. Some of the latter two are apparent septets or apparent dectets, respectively, when the two J_{FF} values are similar. The time-averaged $^7J_{FF}$ values for the quartets range from 11.3 to 14.7 Hz (the slow-exchange values, which were not observed in this study, would range from 102(2) to 132(2) Hz; the precision of the time-averaged J_{FF} values in this study is ±0.2 Hz). The J_{FF} coupling in fullerene$(CF_3)_n$ compounds is primarily due to direct lone pair−lone pair interactions between proximate F atoms on CF_3 groups that share the same hexagon (i.e., "through-space" Fermi-contact coupling).[21,25,30,46−50] The ^{19}F δ and J_{FF} values reported here are similar to those reported for the other nine characterized $C_{60}(CF_3)_n$ compounds with $n \leq 12$, indicating that the CF_3 addition patterns of **8-1**, **8-2**, **8-3**, **8-4**, **8-5**, **10-4**, **10-5**, **10-6**, and **12-3** are almost certainly combinations of isolated *p*-$C_6(CF_3)_2$ hexagons and/or ribbons or loops of edge-sharing *m*- and *p*-$C_6(CF_3)_2$ hexagons on the surface of C_{60} (each shared edge has one sp^3 carbon atom and therefore one CF_3 group).[19,21,25,28,30] This was proven recently by X-ray crystallography for **8-1**, **8-2**, **10-2**, **10-3**, **10-4**, **10-6**, **12-1**, **12-2**, and **12-3** (see Table 1) and was similarly proven in the current study for **10-5** (see below). Alternative addition patterns for **8-3**, **8-4**, and **8-5** with CF_3 groups on adjacent cage C atoms, as in **6-2**,[21] or with one or more 1,3-$C_5(CF_3)_2$ pentagons, as in **10-3**[25] and **12-2**,[28] can be ruled out because these structural units have unique NMR signatures that are absent from the spectra of **8-3**, **8-4**, and **8-5**.

The ^{19}F NMR spectra of **8-2**, **8-3**, and **8-5** each include four quartets, two of which have the same J_{FF} value (12.4 Hz for **8-2**, 12.0 Hz for **8-3** and 11.5 Hz for **8-5**), indicative of a ribbon of six CF_3 groups plus an isolated *p*-$C_6(CF_3)_2$ hexagon and overall C_1 symmetry. The $^7J_{FF}$ coupling constants for the terminal CF_3 quartets on the ribbon in each compound, which are 12.0 and 13.2 Hz for **8-2** and 11.3 and 14.7 Hz for both **8-3** and **8-5**, are similar to the $^7J_{FF}$ values for the CF_3 groups at the termini of the p^3mp ribbon in **6-1**, 11.4 and 14.0 Hz.[19] This strongly suggests that the ribbons of six CF_3 groups in these two isomers of $C_{60}(CF_3)_8$ are p^3mp ribbons, not *pmpmp* ribbons. In the case of **8-2**, this was proven by X-ray crystallography.[24] The particular p^3mp,p isomers that we have assigned to **8-3** and **8-5**, which are shown as Schlegel diagrams in Figure 1, are based on an analysis of their ^{19}F NMR spectra (see Figure S-5) and on their DFT-predicted relative energies (see Table S-2).

The ^{19}F NMR spectra of **8-4** and **10-5** are similar in that they exhibit only two quartets, indicative of a single ribbon of seven and nine edge-sharing *m*- or *p*-$C_6(CF_3)_2$ hexagons, respectively, and overall C_1 symmetry. Furthermore, the $^7J_{FF}$ values for the quartets, 11.7 and ca. 12 Hz for **8-4** and 11.3 and 12.0 Hz for **10-5**, are more similar to one another than is the case for ribbons that have a p^3 end and a *pmp* end. The structure of **10-5** is now known to have a *pmpmpmpmp* addition pattern (this work), and we therefore propose that the structure of **8-4** has a *pmpmpmp* addition pattern. This assignment is also supported by its low relative energy (see Table S-2).

X-ray Crystallography. A drawing of the structure of **10-5**, with thermal ellipsoids for the CF_3 groups and the cage carbon atoms to which they are attached, is shown in Figure 2. Other drawings showing thermal ellipsoids and IUPAC lowest-locant numbering for all atoms are in the SI (Figures S-6 and S-7). In harmony with the ^{19}F NMR spectra, the CF_3 groups are found along ribbons of edge-sharing *p*- and *m*-$C_6(CF_3)_2$ hexagons. The addition pattern of **10-5** is a *pmpmpmpmp* ribbon.

The X-ray structures of the other $C_{60}(CF_3)_n$ derivatives listed in Table 1 have shown that ribbons of edge-sharing *p*- and *m*-$C_6(CF_3)_2$ hexagons lead to a number of very short $C(sp^2)-C(sp^2)$ pentagon−hexagon junctions (PHJs) in the fullerene cage, in

(45) Sheldrick, G. M. *SHELXTL*, v. 6.14; Bruker AXS: Madison, WI 2004.
(46) Kareev, I. E.; Santiso-Quinones, G.; Kuvychko, I. V.; Ioffe, I. N.; Goldt, I. V.; Lebedkin, S. F.; Seppelt, K.; Strauss, S. H.; Boltalina, O. V. *J. Am. Chem. Soc.* **2005**, *127*, 11497−11504.
(47) Alkorta, I.; Elguero, J. E. *Struct. Chem.* **2004**, *15*, 117−120.
(48) Ernst, L.; Ibrom, K. *Angew. Chem., Int. Ed.* **1995**, *34*, 1881−1882.
(49) Arnold, W. D.; Mao, J.; Sun, H.; Oldfield, E. *J. Am. Chem. Soc.* **2000**, *122*, 12164−12168.
(50) Dorozhkin, E. I.; Ignat'eva, D. V.; Tamm, N. B.; Goryunkov, A. A.; Khavrel, P. A.; Ioffe, I. N.; Popov, A. A.; Kuvychko, I. V.; Streletskiy, A. V.; Markov, V. Y.; Spandl, J.; Strauss, S. H.; Boltalina, O. V. *Chem. Eur. J.* **2006**, *12*, 3876−3889.

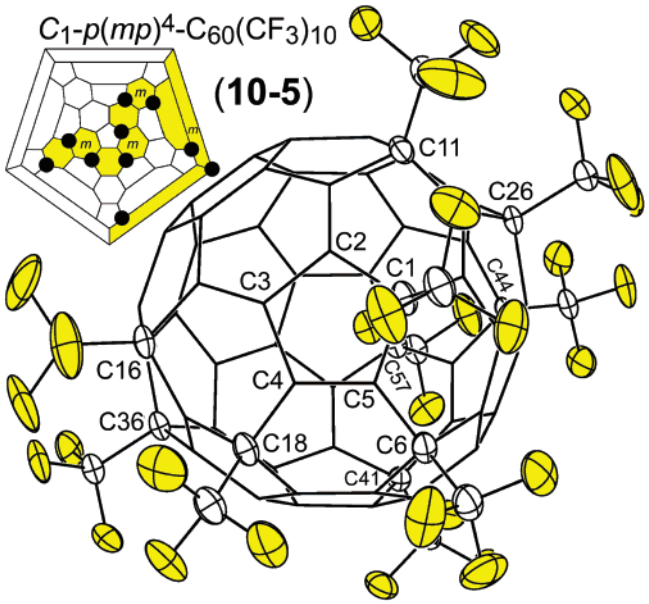

Figure 2. Drawings of the structure of **10-5** (C_1-*pmpmpmpmp*-$C_{60}(CF_3)_{10}$ (50% probability ellipsoids for the CF_3 groups and the cage carbon atoms to which they are attached). The IUPAC lowest locants are shown for some cage carbon atoms (note that this orientation is not the same as in the Schlegel diagram for this compound in some of the other figures). See Supporting Information for drawings showing the numbering of all atoms.

contrast to the long PHJs in C_{60}, which are 1.45 ± 0.01 Å.[51] There are five double bonds in pentagons (DBIPs), which are generally considered to be destabilizing:[52,53] C4−C5, 1.352(3) Å; C9−C10, 1.352(3) Å; C17−C37, 1.345(3) Å; C27−C45, 1.355(3) Å; and C42−C43, 1.345(3) Å. These are of two types: (i) terminal DBIPs (*t*-DBIPs) that have only one C(sp^2) nearest neighbor and (ii) non-terminal DBIPs (*nt*-DBIPs) that have a pair of C(sp^2) nearest neighbors. Only the double bond is an *nt*-DBIP. This distinction will become important in the Discussion section. The cage C−C distances involving two sp^2 C atoms in the structure of **10-5** are shown in Figure S-7 (see SI).

As in the structures of other fullerene$(CF_3)_n$ structures with ribbon addition patterns, there is a network of F···F contacts between F atoms of CF_3 groups that share the same hexagon in **10-5**. These range from 2.522(3) to 2.678(3) Å. None of the CF_3 groups in the structure of **10-5** is eclipsed with respect to the three cage C atoms that radiate from the cage C atom to which the CF_3 group is attached. That observation is consistent with the lack of any ^{19}F NMR multiplets with δ values less than 60 ppm, which is the hallmark of eclipsed CF_3 groups.[28,30]

Electronic and Fluorescence Spectra. Peak maxima and the low-energy onsets of absorption from the electronic absorption spectra of the 18 compounds with $n \leq 12$ are listed in Table 3 along with relevant data for some other $C_{60}(X)_n$ compounds.[54−58] Absorption and emission spectra of four of the six isomers of $C_{60}(CF_3)_{10}$ are shown in Figure 3 (the fluorescence spectrum of **10-1** was not recorded), and absorption spectra of the other $C_{60}(CF_3)_n$ compounds with $n \leq 12$ are shown in Figure S-8 (see SI).

Electrochemical Measurements. Cyclic voltammograms for 10 of the 18 $C_{60}(CF_3)_n$ compounds with $n \leq 12$ are shown in Figures 4 and 5. Additional annotated cyclic voltammograms are shown in Figure S-9 (see SI). The $E_{1/2}$ values for reversible reductions (i.e., quasi-reversible waves with $\Delta E_p \leq 90$ mV for a scan speed of 20 mV s^{-1} and $\Delta E_p \leq 150$ mV for scan speeds greater than or equal to 2.0 mV s^{-1}) are listed in Table 4. Eleven of the 18 compounds exhibited three reversible reductions (the exceptions were **8-5**, **10-2**, **10-3**, **10-6**, **12-1**, **12-2**, and **12-3**). The compounds **8-5** and **12-1** each exhibited only one quasi-reversible reduction. In a few cases (the first reductions of **8-1** and **8-5** and the second reduction of **10-3**), the ratio i_c/i_a was less than one, but the magnitude of i_c and i_a as well as their ratio did not change during multiple scans.

DFT-Predicted Frontier Orbitals for $C_{60}(CF_3)_n$ Compounds and $C_{60}(CF_3)_n^-$ Radical Anions. The PBE-predicted relative energies of the Kohn−Sham HOMOs and LUMOs for the 22 real and four hypothetical $C_{60}(CF_3)_n$ compounds studied are listed in Table 4. Drawings of these orbitals for **10-4**, **12-1**, **16-2**, and **18-1** are shown in Figure S-10 (see SI). The singly occupied molecular orbitals (SOMOs) of the $C_{60}(CF_3)_n^-$ radical anions are topologically virtually identical to the LUMOs of the corresponding $C_{60}(CF_3)_n$ neutral compounds, as shown for **6-2**, **8-1**, and **10-5** in Figure S-11 (see SI). In addition, Figure 6 also includes a Schlegel representation of the SOMO for the **6-1**$^-$ radical anion. The blue (+) and green (−) circles represent the upper lobes of the π atomic orbitals for each cage carbon atom scaled approximately to their contributions to the SOMO. Furthermore, the relative LUMO and SOMO energies are, as expected, strongly correlated, as shown in Figure S-12 (see SI).

The DFT-predicted LUMO energies for $C_{60}(X)_n$ species with the same addition patterns as those of **2-1**, **4-1**, **6-1**, **8-1**, and **10-2** for X = CH_3, Ph, H, NH_2, CH_2F, CHF_2, CF_3, F, NO_2, and CN are shown graphically in Figure 6, and those for $C_{60}(X)_n$ species with the same addition patterns as those of **6-2**, **10-1**, and **12-2** for the same ten substituents are shown in Figure S-13 (see SI). For the addition patterns in Figure 6, there is a monotonic increase in *E*(LUMO) from $n = 2$ to $n = 10$ for X = CH_3, Ph, H, NH_2, and CH_2F and a monotonic decrease in *E*(LUMO) from $n = 2$ to $n = 10$ for X = CF_3, F, NO_2, and CN. Interestingly, the *E*(LUMO) values for all five addition patterns are nearly the same for X = CHF_2.

As might be expected, the LUMO energies for the $C_{60}(X)_n$ compounds are correlated with both gas-phase electron affinities (*EA*s) of *m*-X-$C_6H_4NO_2$ compounds[59] and group electronegativities[60] of the substituents X calculated from benzene deformations, as shown in Figure S-14 (see SI) for the addition pattern of **10**−**2** with X = CH_3, H, NH_2, CF_3, F, NO_2, and CN. The trends are not strictly monotonic, however, possibly because the substituents are attached to C(sp^3) atoms in $C_{60}X_n$ derivatives

(51) Olmstead, M. M.; de Bettencourt-Dias, A.; Lee, H. M.; Pham, D.; Balch, A. L. *Dalton Trans.* **2003**, 3227−3232.
(52) Matsuzawa, N.; Dixon, D. A.; Fukunaga, T. *J. Phys. Chem.* **1992**, *96*, 7594−7604.
(53) Matsuzawa, N.; Fukunaga, T.; Dixon, D. A. *J. Phys. Chem.* **1992**, *96*, 10747−10756.
(54) Gonzalez, R.; Wudl, F.; Pole, D. L.; Sharma, P. K.; Warkentin, J. *J. Org. Chem.* **1996**, *61*, 5837−5839.
(55) Kadish, K. M.; Gao, X.; Van Caemelbecke, E.; Suenobu, T.; Fukuzumi, S. *J. Phys. Chem. A* **2000**, *104*, 3878−3883.
(56) Kitagawa, T.; Tanaka, T.; Takata, Y.; Takeuchi, K.; Komatsu, K. *J. Org. Chem.* **1995**, *60*, 1490−1491.
(57) Kadish, K.; Gao, X.; Van Caemelbecke, E.; Suenobu, T.; Fukuzumi, S. *J. Am. Chem. Soc.* **2000**, *122*, 563−570.
(58) Coheur, P.-F.; Cornil, J.; dos Santos, D. A.; Birkett, P. R.; Lievin, J.; Bredas, J. L.; Walton, D. R. M.; Taylor, R.; Kroto, H. W.; Colin, R. *J. Chem. Phys.* **2000**, *112*, 8555−8566.
(59) Kebarle, P.; Chowdhury, S. *Chem. Rev.* **1987**, *87*, 513−534.
(60) Campanelli, A. R.; Domenicano, A.; Ramondo, F.; Hargittai, I. *J. Phys. Chem. A* **2004**, *108*, 4940−4948.

Table 3. Electronic Spectral Data for $C_{60}(CF_3)_n$ (n = 2, 4, 6, 8, 10, 12) and Related Compounds[a]

compd	low-energy absorption onset, nm	main absorption features, nm
2-1	730	690, 626, 601, 441, 322, 256
1,7-$C_{60}(CO_2Me)(CH_2CH_2SiMe_3)$[b]		688, 618, 538, 448, 332
1,7-$C_{60}(CH_2Ph)_2$[c]		ca. 690, ca. 610, ca. 540, 445, 329, 256
1,7-$C_{60}(^t$Bu)(R)[d]		ca. 450, ca. 320, ca. 250
4-1	720	672, 610, 568, 529, 450, 350, 318, 253
1,6,11,18-$C_{60}(CH_2Ph)_4$[e]		ca. 690, 464, 364, 304, 250
6-1	700	598, 470, 370, 320
6-2	565	511, 463, 432, 378, 351, 335, 270, 256
1-Cl-6,9,12,15,18-$C_{60}Ph_5$[f]		516, 474, 438, 394, 351, 339, 272, 259
8-1	700	648, 593, 523, 477, 440, 357, 340, 330
8-2	700	655, 580, 544, 474, 410, 380, 313, 265, 248
8-3	710	652, 580, 539, 494, 472, 422, 377, 315, 280
8-4	640	522, 483, 349, 306
8-5	670	622, 540, 482, 457, 390, 362, 321, 290
10-1	800	665, 567, 525, 492, 459, 422, 359, 323, 298
10-2	650	540, 483, 456, 427, 370, 343, 326
10-3	600	601, 485, 454, 421, 323
10-4	750	580, 539, 501, 432, 375, 357, 340
10-5	650	535, 492, 461, 436, 383, 343/331
10-6	640	529, 498, 454, 350, 312, 295, 278
12-1	630	429, 410, 382, 338, 313, 291
12-2	740	637, 613, 596, 545, 470, 378, 360, 328
12-3	500	468, 434, 406, 328, 311

[a] All data from this work unless otherwise noted; all spectra from this work were recorded for dichloromethane solutions. [b] Reference 54. [c] Reference 55. [d] Reference 56. [e] Reference 57. [f] Reference 58; the spectra of the 1-H- and 1-OH- analogues are very similar to the spectrum of the 1-Cl- compound listed here.

and C(sp^2) atoms in substituted benzenes. The LUMO energies follow the order $CH_3 \sim H > NH_2 > CF_3 > F > NO_2 > CN$, the *m*-X-$C_6H_4NO_2$ *EA* values (±0.1 eV) follow the order $NH_2 < CH_3 \sim H < F < CF_3 < CN < NO_2$,[59] and the group electronegativities follow the order $H < CH_3 < NH_2 < CF_3 < CN < F < NO_2$.[60]

ESR Spectra. Experimental and DFT-predicted X-Band ESR spectra of the radical anions C_1-*pmp*-$C_{60}(CF_3)_4^-$ (**4-1**$^-$) and C_1-p^3*mpmpmp*-$C_{60}(CF_3)_{10}^-$ (**10-2**$^-$) are shown in Figure 7. The accompanying Schlegel diagrams depict the B3LYP-predicted SOMO for each compound.

Discussion

New Addition Patterns. Of the 18 $C_{60}(CF_3)_n$ addition patterns with $n \leq 12$, only those for **2-1**, **4-1**, and **6-2** are known with substituents other than CF_3 groups (e.g., 1,7-$C_{60}Bn_2$,[61,62] 1,7-$C_{60}(COOH)(CH_2CH_2SiMe_3)$,[54] 1,7-$C_{60}(t$-BuOO)$_2$,[63] 1,6,11,18-$C_{60}Bn_4$,[57] 1,6,9,12,15,18-$C_{60}Me_6$,[64] and 1,6,9,12,15,18-$C_{60}Br_6$[65]). The p^3mp addition pattern of **6-1** has been observed previously, not only for $C_{60}(CF_3)_6$ (structure determined by ^{19}F NMR spectroscopy[19] and DFT calculations[20]) but also for the C_{60}-like polar region in one of the isomers of $C_{70}(CF_3)_6$ (structure determined by X-ray crystallograpy[31]). Trifluoromethyl groups are sterically bulky (they are significantly larger than iodine atoms, for example[66,67]), and of the compounds with $n \leq 12$ only **6-2** and **12-3** are known to have two CF_3 groups on adjacent cage carbon atoms.[21] Therefore, 1,4 addition appears to be the rule for CF_3 (and C_2F_5) groups, as it is for the addition of Br atoms.[68] Most other classes of C_{60} derivatives made by multiple additions of a single substituent involve 1,2 additions, including hydrofullerenes,[69,70] fluorofullerenes,[69−71] and polycycloadducts.[72] Furthermore, only two of the 18 addition patterns with $n \leq 12$ have two CF_3 groups on the same pentagon (**10-3** has one 1,3-$C_5(CF_3)_2$ pentagon[25] and **12-2** has two of them[28]). It is not surprising, therefore, that five of the seven new compounds reported here have one of the two more common fullerene$(CF_3)_n$ addition patterns, (i) a single ribbon of edge-sharing *m*- and/or *p*-$C_6(CF_3)_2$ hexagons (**8-1** has a p^3mpmp ribbon, **8-4** has a *pmpmpmp* ribbon, and **10-5** has a *pmpmpmpmp* ribbon) or (ii) a ribbon plus an isolated *p*-$C_6(CF_3)_2$ hexagon (**8-3** and **8-5**, like the known structure of **8-2**,[24] both have a variation of the p^3mp,*p* addition pattern, the only difference being the location of the isolated hexagon; **10-1** has a p^3mpmp,*p* addition pattern). The structures of **10-6** and **12-3** are unprecedented but are related to known addition-pattern motifs.

Most of the $C_{60}(CF_3)_n$ addition patterns have not been the subjects of previous computational studies, even with the common substituents H, F, Cl, Br, Me, or Ph. This may be, in part, because most of the $C_{60}(CF_3)_n$ addition patterns are asymmetric, and fullerene theorists have tended to focus on $C_{60}(X)_n$ derivatives with at least one element of symmetry. Another reason, in some cases, may be the frequent assumption that the most stable $C_{60}(X)_{n+2}$ compounds must derive from the most

(61) Kadish, K. M.; Gao, X.; Van Caemelbecke, E.; Hirasaka, T.; Suenobu, T.; Fukuzumi, S. *J. Phys. Chem.* **1998**, *100*, 3898−3906.
(62) Zheng, M.; Li, F.; Shi, Z.; Gao, X.; Kadish, K. *J. Org. Chem.* **2007**, *72*, 2538−2542.
(63) Huang, S.; Xiao, Z.; Wang, F.; Gan, L.; Zhang, X.; Hu, X.; Zhang, S.; Lu, M.; Pan, Q.; Xu, L. *J. Org. Chem.* **2004**, *69*, 2442−2453.
(64) Al-Matar, H.; Abdul-Sada, A. K.; Avent, A. G.; Fowler, P. W.; Hitchcock, P. B.; Rogers, K. M.; Taylor, R. *J. Chem. Soc., Perkin Trans.* **2002**, *2*, 53−58.
(65) Troyanov, S. I.; Popov, A. A.; Denisenko, N. I.; Boltalina, O. V.; Sidorov, L. N.; Kemnitz, E. *Fullerenes Nanotubes Carbon Nanostruct.* **2003**, *11*, 61−77.
(66) Charton, M. *J. Am. Chem. Soc.* **1969**, *91*, 615−618.
(67) Bott, G.; Field, L. D.; Sternhell, S. *J. Am. Chem. Soc.* **1980**, *102*, 5618−5626.
(68) Clare, B. W.; Kepert, D. L. *J. Mol. Struct. (THEOCHEM)* **1995**, *340*, 125−142.
(69) Clare, B. W.; Kepert, D. L. *J. Mol. Struct. (THEOCHEM)* **2002**, *589−590*, 209−227.
(70) Clare, B. W.; Kepert, D. L. *J. Mol. Struct. (THEOCHEM)* **2003**, *621*, 211−231.
(71) Boltalina, O. V.; Strauss, S. H. In *Dekker Encyclopedia of Nanoscience and Nanotechnology*; Schwarz, J. A., Contescu, C., Putyera, K., Eds.; Marcel Dekker: New York, 2004; pp 1175−1190.
(72) Hirsch, A.; Brettreich, M. *Fullerenes*: *Chemistry and Reactions*; Wiley-VCH: Weinheim, 2005.

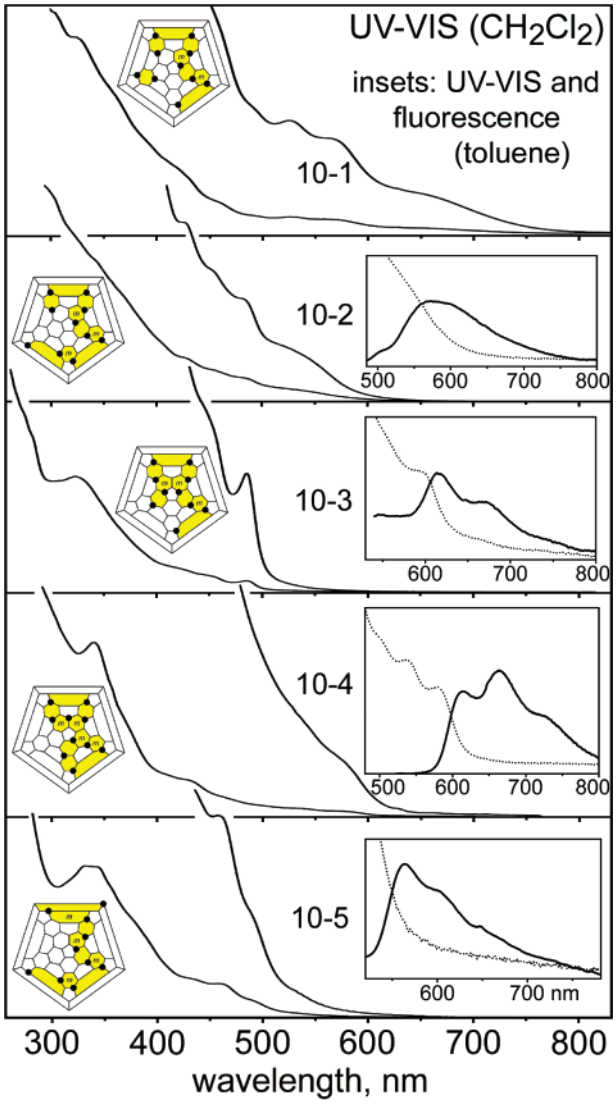

Figure 3. Absorption and emission spectra of toluene solutions of five isomers of $C_{60}(CF_3)_{10}$. The expansion factor is not the same for each spectrum. The insets show portions of the absorption spectra (dotted lines) and the emission spectra (solid lines). Absorption spectra of the other 13 compounds that were investigated can be found in the Supporting Information.

stable $C_{60}(X)_n$ derivatives by simply adding two more X substituents with no rearrangement (e.g., this assumption was made in recent computational studies of $C_{60}Cl_n$ isomers[73] and $C_{60}F_n$ isomers[74]). This assumption, however, has been challenged recently, both on theoretical grounds[75] and in a recent study of $C_{60}F_8$ isomers.[76]

Absorption and Emission Spectra, Optical Gaps, and DFT-predicted HOMO−LUMO Gaps. The UV−vis spectra of exohedral fullerene derivatives *of a fixed composition* are strongly sensitive to the addition pattern of the substituents[58,77−79]

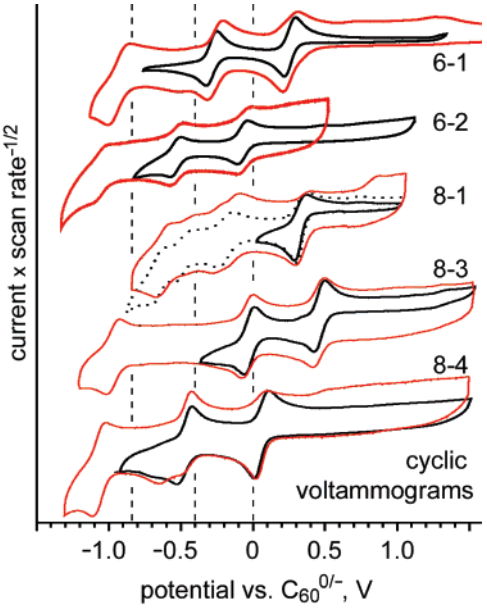

Figure 4. Cyclic voltammograms of the two isomers of $C_{60}(CF_3)_6$ and three of the five isomers of $C_{60}(CF_3)_8$ (0.10 M $TBA^+BF_4^-$ in CH_2Cl_2; the scan rate for the black voltammograms was 20 mV s^{-1}; the scan rates for the red voltammograms were 5.0 V s^{-1} for **6-1**, 3.5 V s^{-1} for **6-2**, and 2.0 V s^{-1} for **8-1**, **8-2**, and **8-3**; $E_{1/2}(C_{60}^{0/-}) = -0.98$ or -0.46 V vs $Fe(Cp)_2^{+/0}$ or $Fe(Cp^*)_2^{+/0}$ internal standards, respectively). The vertical dotted lines show the first, second, and third reduction $E_{1/2}$ values for C_{60} under identical conditions. Slow- and fast-scan-rate cyclic voltammograms for all of the compounds investigated are collected in the Supporting Information.

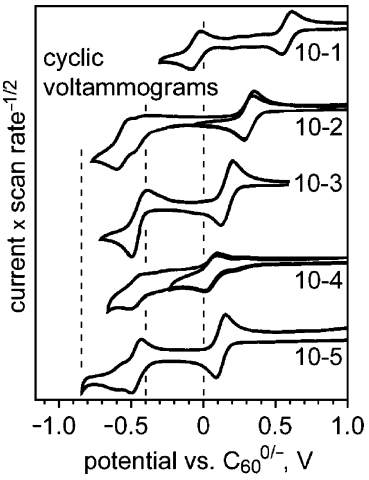

Figure 5. Cyclic voltammograms of five of the six isomers of $C_{60}(CF_3)_{10}$ (0.10 M $TBA^+BF_4^-$ in CH_2Cl_2; the scan rate was 20 mV s^{-1}; $E_{1/2}(C_{60}^{0/-}) = -0.98$ or -0.46 V vs $Fe(Cp)_2^{+/0}$ or $Fe(Cp^*)_2^{+/0}$ internal standards, respectively). The vertical dotted lines show the first, second, and third reduction $E_{1/2}$ values for C_{60} under identical conditions.

but, except for minor shifts in λ_{max} values of a few nm, are not sensitive to the electronic properties of the substituents unless the substituents themselves are chromophores. This can be readily seen in Table 3 by comparing the λ_{max} values for **2-1** with those for 1,7-$C_{60}(C_6H_5CH_2)_2$ and 1,7-$C_{60}(COOCH_3)$-$(SiMe_3)$, the λ_{max} values for **4-1** with those for 1,6,11,18-C_{60}-Bn_4, and the λ_{max} values for **6-2** with those for 1-Cl-6,9,12,15,18-$C_{60}Ph_5$ (the low-energy absorptions of 1,6,11,18-$C_{60}Bn_4$ were not reported in the original paper,[57] but we recently learned that the lowest energy absorption occurs at ca. 690 nm for this compound [X. Gao, personal communication, 2007]). In addition, the ranges of DFT-predicted HOMO−LUMO gaps for the

(73) Liang, Y.; Shang, Z.; Wang, G.; Cai, Z.; Pan, Y.; Zhao, X. *J. Mol. Struct. (THEOCHEM)* **2004**, *677*, 15−19.
(74) Van Lier, G.; Cases, M.; Ewels, C. P.; Taylor, R.; Geerlings, P. *J. Org. Chem.* **2005**, *70*, 1565−1579.
(75) Sandall, J. P. B.; Fowler, P. W. *Org. Biomol. Chem.* **2003**, *1*, 1061−1066.
(76) Goryunkov, A. A.; et al. *J. Fluorine Chem.* **2006**, *127*, 1423−1435.
(77) Foley, S.; Bosi, S.; Larroque, C.; Prato, M.; Janot, J.-M.; Seta, P. *Chem. Phys. Lett.* **2001**, *350*, 198−205.
(78) Kordatos, K.; Bosi, S.; da Ros, T.; Zambon, A.; Lucchini, V.; Prato, M. *J. Org. Chem.* **2001**, *66*, 2802−2808.
(79) Marchesan, S.; da Ros, T.; Prato, M. *J. Org. Chem.* **2005**, *70*, 4706−4713.

Table 4. Experimental and DFT Results for $C_{60}(CF_3)_n$ Derivatives (n = 2, 4, 6, 8, 10, 12, 16, 18)

		DFT		relative $E_{1/2}$, V vs $C_{60}^{0/-}$ [a]		
cmpd	exptl λ_{max}, eV (nm)[b]	E(HOMO) − E(LUMO), eV (vs C_{60}, eV)[c]	E(LUMO), eV (vs C_{60}, eV)[c]	0/−	−/2−	2−/3−
C_{60}	1.95 (637)	1.639 (0.000)	−4.379 (0.000)	0.00 {0.46}	−0.40 {0.06}	−0.84 {−0.38}
2-1	1.79 (690)	1.430 (−0.209)	−4.592 (−0.213)	0.11 [*0.09*]	−0.30 [*−0.32*]	−0.83
4-1	1.85 (672)	1.443 (−0.196)	−4.682 (−0.303)	0.17 [*0.16*]	−0.26 [*−0.26*]	−1.01[d]
6-1	2.08 (598)	1.445 (−0.194)	−4.796 (−0.417)	0.26 [*0.26*]	−0.28 [*−0.27*]	−0.93[e]
6-2	2.43 (511)	1.859 (+0.220)	−4.378 (+0.001)	−0.07 [*−0.08*]	−0.53 [*−0.52*]	−1.02[f]
6-3-CF$_3$		1.381 (−0.258)	−4.858 (−0.479)	[*0.31*]		
6-4-CF$_3$[g]		1.076 (−0.563)	−5.020 (−0.641)	[*0.44*]		
8-1	1.92 (648)	1.498 (−0.141)	−4.850 (−0.471)	0.33 [*0.30*]	−0.19[h] [*−0.25*]	ca. −0.66[h,i]
8-2	1.90 (655)	1.482 (−0.157)	−4.912 (−0.533)	0.32 [*0.35*]	−0.19 [*−0.18*]	−0.79[h]
8-3	1.90 (652)	1.333 (−0.306)	−5.017 (−0.639)	0.45 [*0.44*]	−0.03 [*−0.06*]	−0.96[h]
8-4	2.38 (522)	1.701 (+0.062)	−4.585 (−0.206)	0.06 [*0.09*]	−0.38 [*−0.39*]	−1.06[h]
8-5	2.00 (622)	1.420 (+0.219)	−4.863 (−0.486)	0.31 [*0.31*]	[*−0.21*]	
8-6-CF$_3$		1.302 (−0.337)	−4.895 (−0.516)	[*0.34*]		
10-1	1.87 (665)	1.139 (−0.500)	−5.129 (−0.749)	0.57 [*0.53*]	−0.07 [*−0.03*]	−1.10[f]
10-2	2.30 (540)	1.550 (−0.089)	−4.894 (−0.515)	0.32 [*0.34*]	−0.47[f] [*−0.41*]	
10-3	2.06 (601)	1.662 (−0.023)	−4.754 (−0.375)	0.17 [*0.22*]	−0.44 [*−0.47*]	
10-4	2.14 (580)	1.636 (+0.003)	−4.529 (−0.150)	0.07 [*0.04*]	−0.47 [*−0.43*]	−1.07[f]
10-5	2.32 (535)	1.748 (+0.109)	−4.638 (−0.259)	0.12 [*0.13*]	−0.46 [*−0.48*]	−0.90[f]
10-6	2.34 (529)	1.445 (−0.194)	−4.922 (−0.543)	0.33 [*0.36*]	−0.34[j] [*−0.30*]	
12-1	2.90 (429)	2.245 (+0.606)	−4.278 (+0.101)	−0.16 [*−0.21*]	[*−0.58*]	
12-2	1.87 (662)	1.614 (−0.025)	−4.919 (−0.540)	0.32 [*0.36*]	−0.39 [*−0.33*]	
12-3[k]	2.65 (468)	2.086 (+0.447)	−4.331 (+0.048)	−0.13 [*−0.12*]	−0.59 [*−0.55*]	
16-1		1.798 (+0.159)	−4.792 (−0.413)	[*0.25*]	[*−0.25*]	
16-2		2.254 (+0.615)	−4.533 (−0.154)	[*0.04*]	[*−0.43*]	
16-3		1.897 (+0.258)	−4.810 (−0.431)	[*0.27*]	[*−0.45*]	
18-1		1.787 (+0.148)	−4.848 (−0.469)	[*0.30*]	[*−0.23*]	
18-2-CF$_3$		2.104 (+0.465)	−4.928 (−0.549)	[*0.37*]	[*−0.18*]	

[a] Reversible wave observed at 20 mV s^{-1} unless otherwise noted; electrolyte = 0.10 M N(n-Bu)$_4$BF$_4$ in dichloromethane; $Fe(Cp)_2^{+/0}$ or $Fe(Cp^*)_2^{+/0}$ internal standard ($E_{1/2}$ = −0.46 or −0.98 V vs $C_{60}^{0/-}$, respectively). The values shown in braces are $E_{1/2}$ values vs $Fe(Cp)_2^{+/0}$. The values shown in italics in square brackets are (i) PBE-predicted 0/− $E_{1/2}$ values vs $C_{60}^{0/-}$ based on a correlation with LUMO energies or (ii) B3LYP-predicted −/2− $E_{1/2}$ values vs $C_{60}^{0/-}$ based on a correlation with the sum of second electron affinities plus $\Delta\Delta G$(solvation). [b] Solvent = dichloromethane. [c] From PBE-DFT-predicted HOMO and LUMO energies. [d] Scan rate = 200 mV s^{-1}. [e] Scan rate = 5.0 V s^{-1}. [f] Scan rate = 3.5 V s^{-1}. [g] The **6-4** addition pattern, 1,23,28,33,38,60-$C_{60}(X)_6$, has only been observed for X = CMe(COOCMe$_3$)$_2$ (see Figure S-3 in the Supporting Information for the Schlegel diagram of this compound). [h] Scan rate = 2.0 V s^{-1}. [i] The 2−/3− $E_{1/2}$ value for **8-1** was not precisely determined because the third reduction wave was poorly defined. [j] Scan rate = 100 mV s^{-1}. [k] This product may be a mixture of up to three isomers, all with two skew-pentagonal-pyramidal arrays of six CF_3 groups on opposite C_{60} poles.

compounds in Figure 6 with X = CH_3, Ph, CH_2F, CHF_2, CF_3, and CN are only 0.013, 0.032, 0.044, 0.063, and 0.137 eV for the **2-1**, **4-1**, **6-1**, **8-1**, and **10-2** addition patterns, respectively. In addition, a DFT-predicted 0.084 eV range of HOMO−LUMO gaps was recently reported[34] for the set of compounds 1,23,-28,33,38,60-$C_{60}(X)_6$ with X = CH_3, CH_2F, CHF_2, CF_3, and CBr(COOEt)$_2$ and CMe(COOMe)$_2$ (the compound with X = CMe(COOCMe$_3$)$_2$ is known and has been structurally characterized[33]). Therefore, the electronic absorption spectra reported herein may prove useful in the future for the elucidation of structures of other $C_{60}(X)_n$ derivatives with bulky substitutents.

Absorption spectra for the 18 $C_{60}(CF_3)_n$ compounds are reported here for the first time except for those of **2-1** and **6-2** ($n \leq 12$). The emission spectra of **10-2**, **10-3**, **10-4**, and **10-5** are also reported here for the first time. The optical gaps for the $C_{60}(CF_3)_n$ compounds, which correspond to the lowest-energy absorption feature in each spectrum, do not steadily increase as n increases, unlike the situation with the series of methanofullerenes $C_{60}(CR_1R_2)_n$ (n = 1−6), for which the longest-wavelength λ_{max} value does decrease as n increases).[80] For example, the lowest-energy absorptions of **2-1**, **4-1**, **8-1**, **8-3**, and **10-1** are red-shifted relative to C_{60}, and the analogous absorptions of **6-1**, **6-2**, **8-4**, **10-2**, **10-3**, **10-4**, and **10-5** are blue-shifted relative to C_{60}. More specifically, the spectra of the five isomers of $C_{60}(CF_3)_{10}$ shown in Figure 3 are different from one another in (i) the onset of absorption and (ii) the number of detectable features. The range of optical gaps for these five isomers is 0.69 eV, the range for the five isomers of $C_{60}(CF_3)_8$ is 0.48 eV, and the optical gaps for the two isomers of $C_{60}(CF_3)_6$ and two isomers of $C_{60}(CF_3)_{12}$ differ by 0.35 and 1.03 eV, respectively. These are extremely large optical-gap ranges for isomers of C_{60} derivatives with a given composition. In contrast, the lowest energy absorption is ca. 690 nm for both 1,9- and 1,7-$C_{60}(Bn)_2$;[55] it ranges from 696 to 721 nm (Δgap = 0.06 eV) for six regioisomers of bis(pyrrolidine) adducts of C_{60},[81] and it ranges from 650 to 720 nm (Δgap = 0.19 eV) for nine tris(*N*-methylpyrrolidine) adducts of C_{60}.[79] Even for isomers of pentakis-cycloadducts of C_{60} (the functional equivalent of $C_{60}(X)_{10}$ derivatives), the spectra of which were previously described as differing "distinctly from one another," the range of optical gaps reported was only 0.15 eV.[80]

Nevertheless, in addition to the work reported herein, there are two previous examples for which relatively large optical-gap ranges (i.e., ≥ 0.25 eV) for isomeric $C_{60}(X)_n$ derivatives can be inferred. The first example is a study of hexakis-cycloadduct derivatives of C_{60} with different addition patterns (the functional equivalent of of $C_{60}(X)_{12}$ derivatives). Although the substituents are not identical (and therefore the compounds are not strictly isomeric), the lowest energy absorption varied

(80) Cardullo, F.; Seiler, P.; Isaacs, L.; Nierengarten, J.-F.; Haldimann, R. F.; Diederich, F.; Mordasini-Denti, T.; Thiel, W.; Boudon, C.; Gisselbrecht, J. P.; Gross, M. *Helv. Chim. Acta* **1995**, *80*, 343−371.

(81) Kordatos, K.; da Ros, T.; Prato, M.; Bensasson, R. V.; Leach, S. *Chem. Phys.* **2003**, *293*, 263−280.

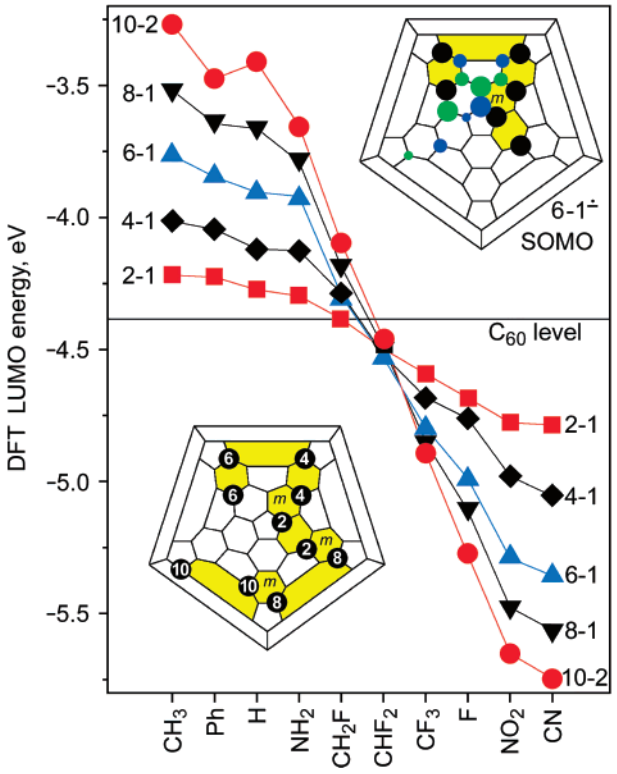

Figure 6. DFT-predicted LUMO energies for single-substituent $C_{60}(X)_n$ derivatives with the same addition patterns as **2-1**, **4-1**, **6-1**, **8-1**, and **10-2** and with a variety of X substituents. The Schlegel diagram in the lower-left corner shows the five addition patterns used for each substituent. The addition pattern for **10-2** is all ten black circles; the addition pattern for **8-1** is all black circles except for the two labeled "**10**"; etc. The Schlegel diagram in the upper-right corner shows the singly occupied molecular orbital (SOMO) for the **6-1**$^-$ radical anion with CF_3 groups. The blue (+) and green (−) circles represent the upper lobes of the π atomic orbitals for each cage carbon atom scaled approximately to their contributions to this orbital. The SOMO for the **8-1**$^-$ radical anion with CF_3 groups is nearly identical to the **6-1**$^-$ SOMO.

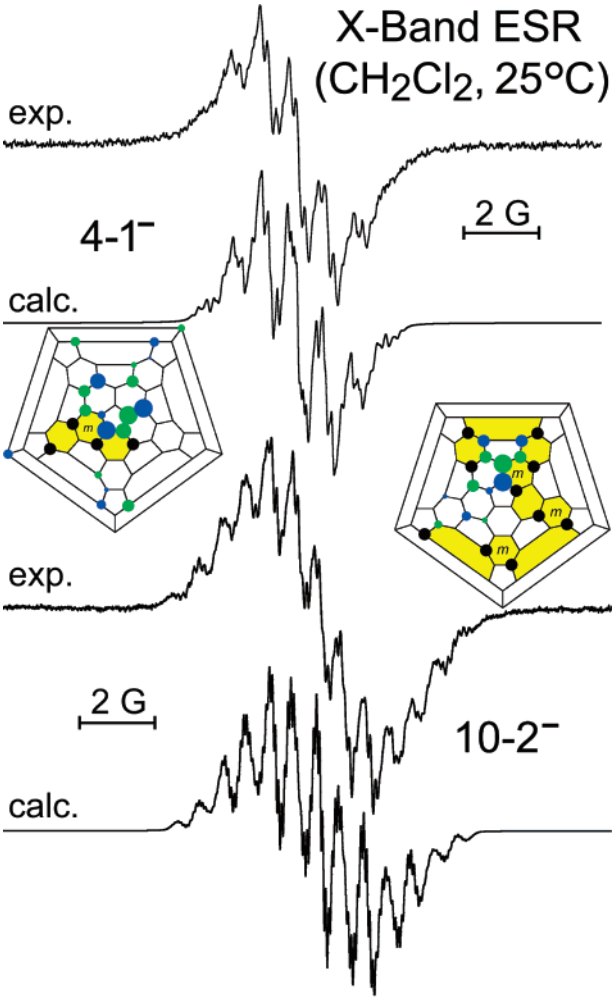

Figure 7. Experimental (dichloromethane, 25 °C) and DFT-predicted X-Band ESR spectra of the radical anions C_1-*pmp*-$C_{60}(CF_3)_4^-$ (**4-1**$^-$; dichloromethane) and C_1-p^3*mpmpmp*-$C_{60}(CF_3)_{10}^-$ (**10-2**$^-$; *o*-dichlorobenzene). The DFT-computed hyperfine coupling constants were uniformly scaled by 0.9 in order to match the experimental values. The Schlegel diagrams show the B3LYP-predicted singly occupied molecular orbital (SOMO) for each compound. The blue (+) and green (−) circles represent the upper lobes of the π atomic orbitals for each cage carbon atom scaled approximately to their contributions to the SOMO.

from 600 to 450 nm (Δgap = 0.69 eV).[82] The second example is the emerald-green compound 1,23,28,33,38,60-C_{60}(CMe(COOCMe$_3$)$_2$)$_6$, which has an intense band at 850 nm and a lowest energy absorption at 1170 nm.[33] If the substituent effect on the optical gap is ignored, the difference between the lowest energy absorption of this compound and the 516-nm onset of absorption of 1-Cl-6,9,12,15,18-$C_{60}Ph_5$[58] results in a Δgap value of 1.34 eV. Finally, as part of this work, we recorded the absorption spectra of the two isomers of $C_{60}F_8$,[76] and these are shown in Figure S-15. The lowest energy absorption are ca. 650 nm and ca. 575 nm, resulting in a Δgap value of 0.25 eV.

To confirm that the lowest-energy feature in the absorption spectrum (i.e., the optical gap) of a given $C_{60}(CF_3)_n$ derivative may, in general, be unambiguously assigned to the HOMO−LUMO transition,[83−89] we measured the emission spectra of four isomers of $C_{60}(CF_3)_{10}$ and compared them with the corresponding absorption spectra (see Figure 3). The emission spectra were independent of the excitation wavelength used, indicating that emission occurs from the S_1 state. It should be noted that the "mirror-image rule" is not always obeyed by fullerene derivatives because of the high density of excited states and the concomitant overlap of multiple absorption bands.[58] Nevertheless, there is a good correlation between the absorption and emission spectra for **10-2**, **10-3**, and **10-4**, confirming the assignment of the HOMO−LUMO transition in these derivatives. The broad featureless band at 567 nm in the emission spectrum of **10-2** can be matched with the analogous broad band in the absorption spectrum at 550 nm. The emission spectra of **10-3** and **10-4** have more structure and are therefore even more convincing. For **10-3**, the emission bands at 615 and 673 nm

(82) Bourgeois, J.-P.; Woods, C. R.; Cardullo, F.; Habicher, T.; Nierengarten, J.-F.; Gehrig, R.; Diederich, F. *Helv. Chim. Acta* **2001**, *84*, 1207−1226.
(83) Coheur, P.-F.; Cornil, J.; dos Santos, D. A.; Birkett, P. R.; Lievin, J.; Bredas, J. L.; Walton, D. R. M.; Taylor, R.; Kroto, H. W.; Colin, R. *J. Chem. Phys.* **2000**, *112*, 6371−6381.
(84) Guldi, D.; Asmus, K. D. *J. Phys. Chem. A* **1997**, *101*, 1472−1481.
(85) Lebedkin, S. F.; Rietschel, H.; Adams, G. B.; Page, J. B.; Hull, W. E.; Hennrich, F. R.; Eisler, H.-J.; Kappes, M. M.; Kratschmer, W. *J. Chem. Phys.* **1999**, *110*, 11768−11778.
(86) Amarantov, S. V.; Bezmelnitsin, V. N.; Boltalina, O. V.; Danailov, M.; Dudin, P. V.; Ryzkov, A. V.; Stankevich, V. G. *Nucl. Instrum. Methods Phys. Res., Sect. A* **2001**, *470*, 318−322.
(87) Green, J., W. H.; Gorun, S. M.; Fitzgerald, G.; Fowler, P. W.; Ceulemans, A.; Titeca, B. C. *J. Phys. Chem.* **1996**, *100*, 14892−14898.
(88) Cramariuc, O.; Hukka, T. I.; Rantala, T. T.; Lemmetyinen, H. *J. Phys. Chem. A* **2006**, *110*, 12470−12476.
(89) Guldi, D. M.; Prato, M. *Acc. Chem. Res.* **2000**, *33*, 695−703.

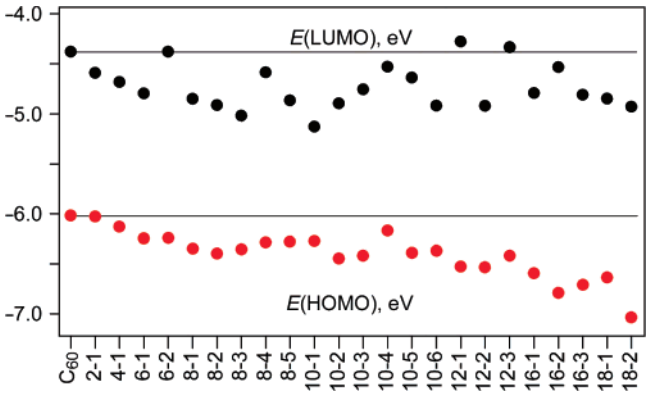

Figure 8. Plot of DFT-predicted Kohn−Sham HOMO and LUMO energies for C_{60} and $C_{60}(CF_3)_n$ derivatives. The horizontal lines are the DFT-predicted HOMO and LUMO energies for C_{60}. The compound **18-2** is not known with CF_3 groups at this time and therefore represents a hypothetical derivative.

(ΔE = 0.175 eV) correspond to the absorption bands at 601 and 554 nm, respectively (ΔE = 0.175 eV); for **10-4**, the emission bands at 613, 664 and 727 nm (ΔE(613/664) = 0.156 eV; ΔE(664/727) = 0.162 eV) correspond to the absorption bands at 584, 540, and 503 nm, respectively (ΔE(584/540) = 0.173 eV; ΔE(540/503) = 0.169 eV). In the case of **10-5**, the main emission band at 563 nm confirms that the 535-nm band in the absorption spectrum, which is better resolved in dichloromethane (not shown) than in toluene, can be assigned to the HOMO−LUMO transition.

Figure S-16 shows a correlation of DFT-predicted HOMO−LUMO gaps with optical gaps for the 18 $C_{60}(CF_3)_n$ derivatives dissolved in dichloromethane. All of the optical gaps are in a region with unit slope and a width of 0.4 eV on the HOMO−LUMO gap axis. The overall correlation between the experimental and calculated frontier-orbital energy gaps is obvious. Deviations of ±0.2 eV from a line of unit slope bisecting the region are not surprising since the HOMO−LUMO gap does not take into account geometric changes of the molecule in the excited state, the possible admixture of other configurations, or solvent effects.[90]

Figure 8 displays the HOMO and LUMO energies for C_{60} and 23 of the compounds listed in Table 4 on the same energy axis. The *E*(HOMO) values become more negative as *n* increases: the average *E*(HOMO) values for the compositions with *n* = 6, 8, 10, 12, and 16 (all real compounds) show a steady decrease except that the average *E*(HOMO) values for *n* = 8 and 10 are nearly the same. On the other hand, the *E*(LUMO) values vary in an irregular way. There is a much larger difference in the range of *E*(LUMO) values for isomers of a given composition than in the range of *E*(HOMO) values. These ranges are: for *n* = 6, ΔE(HOMO) = 0.00 eV, ΔE(LUMO) = 0.42 eV; for *n* = 8, ΔE(HOMO) = 0.12 eV, ΔE(LUMO) = 0.43 eV; for *n* = 10, ΔE(HOMO) = 0.28 eV, ΔE(LUMO) = 0.60 eV; for *n* = 12, ΔE(HOMO) = 0.01 eV, ΔE(LUMO) = 0.64 eV; and for *n* = 16, ΔE(HOMO) = 0.19 eV, ΔE(LUMO) = 0.28 eV (however, the 0.32 eV difference in *E*(HOMO) values for the real compound **18-1** and the hypothetical compound **18-2** is actually larger than the 0.08 eV difference in their *E*(LUMO) values). In addition, DFT calculations for the 24 IPR isomers of C_{84} revealed a range of *E*(HOMO) values, 0.60 eV, only two-thirds as large as the 0.96 eV range of *E*(LUMO) values. Whether this is a general phenomenon for most fullerene(X)$_n$ isomers is not clear at this time. However, it appears to be general for $C_{60}(X)_n$ compounds with the **2-1**, **4-1**, **6-1**, **8-1**, or **10-2** addition patterns for all the substituents X shown in Figure 6. Although the *E*(LUMO) values (and the *E*(HOMO) values) vary by up to 3 eV as the substituent is changed, the HOMO−LUMO gaps only varied by 0.05 eV.

Electrochemical Potentials and DFT-Predicted *E*(LUMO) Values. I. General Comments. All 18 $C_{60}(CF_3)_n$ compounds studied by cyclic voltammetry exhibited reversible first reductions (as defined earlier) at a scan speed of 20 mV s^{-1} in dichloromethane at 25 °C. This is in contrast to many $C_{60}F_n$ compounds, which generally require much higher scan speeds to achieve reversibility or do not exhibit reversible reductions at any scan speed (one exception is $C_{60}F_{48}$, which exhibits a reversible first reduction at 200 mV s^{-1} in dichloromethane at 25 °C).[15,91−94] For reasons that are not clear at this time, some of the $C_{60}(CF_3)_n$ compounds did not exhibit reversible second or third reductions.

However, it is noteworthy that **6-2** exhibited three reversible reductions. The compound 1-Cl-6,9,12,15,18-$C_{60}Ph_5$ (C_s-$C_{60}Ph_5Cl$), with the **6-2** addition pattern, has also been studied electrochemically.[95] Unlike **6-2**, $C_{60}Ph_5Cl$ exhibits an irreversible two-electron reduction, even at −80 °C in dichloromethane, with an cathodic peak potential of −0.09 V vs $C_{60}^{0/-}$.[95] This has been attributed to the following reaction:

$$\text{1-Cl-6,9,12,15,18-}C_{60}Ph_5Cl + 2e^- \rightarrow \text{6,9,12,15,18-}C_{60}Ph_5^- + Cl^-$$

The cyclopentadienyl-like anion C_{5v}-$C_{60}Ph_5^-$ is an especially stable derivative[96,97] and is known to exhibit a reversible one-electron reduction as well as a reversible one-electron oxidation.[98] Interestingly, the compound C_s-$C_{60}Ph_5H$, which also undergoes irreversible reduction at 20 °C, exhibits two reversible reductions at −78 °C in THF.[98] The reversible reductions of **6-2** are probably due to the stronger bonds between the cage and CF_3 groups than between the cage and H or Cl atoms (this may also account for the exceptional thermal stabilities of fullerene$(CF_3)_n$ compounds).

In the remainder of this paper, the discussion of $C_{60}(CF_3)_n$ electrochemical potentials and their comparison to literature values of other $C_{60}(X)_n$ will be limited to *reversible or quasi-reversible potentials* (i.e., $E_{1/2}$ values). Since we are interested in comparing the experimental potentials with calculated LUMO energies, we will omit irreversible reductions in this analysis.

The electrochemical literature on fullerenes and exohedral fullerene(X)$_n$ derivatives is extensive (and many papers also

(90) Armstrong, R. S.; Gallagher, R. T.; Noviandri, I.; Lay, P. A. *Fullerene Sci. Technol.* **1999**, *7*, 1003−1028.
(91) Liu, N.; Touhara, H.; Morio, Y.; Komichi, D.; Okino, F.; Kawasaki, S. *J. Electrochem. Soc.* **1996**, *143*, L214−L217.
(92) Liu, N.; Morio, Y.; Okino, F.; Touhara, H.; Boltalina, O. V.; Pavlovich, V. K. *Synth. Met.* **1997**, *86*, 2289−2290.
(93) Zhou, F.; Van Berkel, G. J.; Donovan, B. T. *J. Am. Chem. Soc.* **1994**, *116*, 5485−5486.
(94) Paolucci, D.; Paolucci, F.; Marcaccio, M.; Carano, M.; Taylor, R. *Chem. Phys. Lett.* **2004**, *400*, 389−393.
(95) Birkett, P. R.; Taylor, R.; Wachter, N.; Carano, M.; Paolucci, F.; Roffia, S.; Zerbetto, F. *J. Am. Chem. Soc* **2000**, *122*, 4209−4212.
(96) Matsuo, Y.; Tahara, K.; Nakamura, E. *Chem. Lett.* **2005**, *34*, 1078−1079.
(97) Sawamura, M.; Nagahama, N.; Toganoh, M.; Hackler, U. E.; Isobe, H.; Nakamura, E.; Zhou, S.-Z.; Chu, B. *Chem. Lett.* **2000**, *29*, 1098−1099.
(98) Iikura, H.; Mori, S.; Sawamura, M.; Nakamura, E. *J. Org. Chem.* **1997**, *62*, 7912−7913.

include computational studies at various levels of theory).[8−13,99] Some studies compared $E_{1/2}$ values (i) for different fullerene cages (e.g., C_{70} vs C_{76}-D_2 vs isomers of C_{78}[100]), (ii) for different substituents with a fixed $C_{60+y}(X)_n$ *n* value and addition pattern (e.g., different monomethano[101,102] or other monoadduct[103] derivatives of C_{60}), and (iii) for different values of *n* with the same substituent, but with only one addition pattern for each value of *n* (e.g., $C_{70}Ph_{2,4,6,8,10}$[104]). Prior to the publication of these $C_{60}(CF_3)_n$ results (some of which were briefly communicated in 2005[15]), there were only a few studies in which two or more $E_{1/2}$ values were compared for *different isomers of a given* $C_{60}(X)_n$ composition, and these are listed in Table 5,[55,57,62,94,105−113] which also includes the ranges for $C_{60}(CF_3)_{6,8,10}$ isomers from this study.

It is clear from the data in Table 5 that well-characterized isomeric $C_{60}(X)_n$ compounds can have ranges of 0/−, 1−/2−, and 2−/3− electrochemical potentials that are significantly larger than previously observed. The $C_{60}(CF_3)_n$ results have set a new standard for comparing the electrochemical potentials of isomeric fullerene compounds. For example, the 0/− $E_{1/2}$ range of 0.07 V for three isomers of $C_{78}(C(COOEt)_2)_3$ previously led to the conclusion that one of the isomers "is *much* more difficult to reduce than the other two derivatives" [emphasis added].[100] The "tunability" of fullerene redox potentials, which is often one of the justifications for the synthesis of new fullerene derivatives,[8,10,11,14,15,62,92,94,99−105,107,114−117] can be as large as 0.5 V for different isomeric exohedral fullerene derivatives of two different compositions ($n = 10$ and 12). This unanticipated result demonstrates the range of electronic compliance of a π system with 20 or more conjugated double bonds on a curved 3-connected network of carbon atoms.

II. Correlation of Electrochemical Potentials with DFT-Predicted LUMO Energies. A plot showing the linear correlation of 0/− $E_{1/2}$ values for the 18 $C_{60}(CF_3)_n$ compounds with $n \leq 12$ with the corresponding PBE-predicted LUMO energies (E(LUMO)) values is shown in Figure 9 ($R^2 = 0.98$; an equally good correlation (not shown; $R^2 = 0.99$) was found for a plot of the same $E_{1/2}$ values vs the B3LYP-predicted LUMO energies). The $E_{1/2}$ and E(LUMO) values in Figure 9 vary from −0.16 to 0.57 V vs $C_{60}^{0/-}$ ($\Delta = 0.73$ V) and from 0.101 to −0.749 eV vs C_{60} ($\Delta = 0.850$ eV), respectively. Linear 0/− $E_{1/2}$ vs E(LUMO) plots have been previously reported in at least three electrochemical studies of fullerene cycloadducts.[14,80,118] In two of these studies, the range of $E_{1/2}$ values was less than or equal to 0.20 V.[14,118] In the third study, the range of $E_{1/2}$ values was ca. 0.8 V, and the E(LUMO) values were determined for simpler model compounds with H atoms and CH_2 groups representing the actual cycloaddition moieties.[80] A fourth paper described an electrochemical study of higher fullerenes and included a plot of [E(HOMO) − E(LUMO)] vs [$E_{1/2}$(ox) − $E_{1/2}$(red)] values, but a simple plot of 0/− $E_{1/2}$ vs E(LUMO) values was not shown.[119]

With $E_{1/2}$ values for multiple isomers of $C_{60}(CF_3)_6$, $C_{60}(CF_3)_8$, $C_{60}(CF_3)_{10}$, and $C_{60}(CF_3)_{12}$, it is now clear that, in general, electrochemical potentials are not a monotonic function of *n*, the number of CF_3 radicals that were added to C_{60}. A plot of the 18 experimental $C_{60}(CF_3)_n$ 0/− $E_{1/2}$ values vs *n* is shown in the inset in Figure 9. Also included in the inset are 0/− $E_{1/2}$ values for **4-2-CF$_3$** and **6-3-CF$_3$**, calculated using the linear least-squares equation shown in the 0/− $E_{1/2}$ vs E(LUMO) plot

Table 5. Experimental $E_{1/2}$ Values for Isomeric $C_{60+y}(X)_n$ Derivatives[a]

$C_{60+y}(X)_n$	no. of isomers	0/− $E_{1/2}$ range, V	−/2− $E_{1/2}$ range, V	2−/3− $E_{1/2}$ range, V
C_{84}[b]	6	0.36	0.33	0.31
C_{78}[c,d]	2	0.06	0.10	0.02
$C_{78}(C(COOEt)_2)_3$[c,e]	3	0.07	0.06	−[f]
$C_{70}(COOCH_2COOMe)_2$[c]	3	0.04	0.02	0.05
$C_{70}H_2$[g]	2	0.01	0.04	0.03
$C_{70}Bn_2$[h]	3	0.15	0.10	0.00
C_{70}(*c*-ONCR)[i]	3	ca. 0	ca. 0	ca. 0
C_{60}(*c*-CH_2N(TEG)$CH_2)_2$[j]	8	0.14	0.15	0.11
$C_{60}F_{36}$[k]	3	0.08		
$C_{60}Me_2$[l]	2	0.00	0.00	0.00
$C_{60}(CH_2Ph)_2$[m]	2	0.01	0.05	0.05
$C_{60}(CH_2Ph)_4$[n]	2	0.05	0.03	0.03
$C_{60}(C(CO_2Et)_2)_3$[o]	7	0.16	0.08	
1,2- vs 1,9-C_{60}(CRR′)[p]	4 pairs	0.11, 0.03, 0.14, 0.09	[0.20], [0.22], [0.18], [0.23][q]	[0.19], [0.19], [0.16], [0.25][r]
1,2- vs 1,9-C_{60}(CRR′)[s]	2	0.01	0.01	0.05
$C_{60}(CF_3)_6$	2	0.33	0.25	0.09
$C_{60}(CF_3)_8$	5	0.39	0.35	0.40[u]
$C_{60}(CF_3)_{10}$	6	0.50	0.40[t]	0.20[u]
$C_{60}(CF_3)_{12}$	2	0.49		

[a] The $C_{60}(CF_3)_n$ data are from this work; only ranges of reversible potentials are listed; the literature $E_{1/2}$ values were generally listed as ±0.01 V. [b] Six cage isomers; ref 109. [c] Reference 100. [d] C_{2v} and D_3 cage isomers. [e] Different cage and addition-pattern isomers. [f] This range, reported to be 0.34 V, is complicated by the facts that the third reduction for one isomer was not reversible and was badly resolved for another isomer. [g] Reference 113. [h] 3,4 and 15,16 isomers; ref 108. [i] Reference 112. [j] Reference 105. [k] C_1, C_3, and *T* isomers; ref 94. [l] Reference 106. [m] 1,9 and 1,7 isomers; ref 62. [n] 1,6,11,18 and 1,6,9,18 isomers; ref 57. [o] Reference107. [p] Reference 110. [q] These $E_{1/2}$ ranges are for the 1+/0 couples. [r] These $E_{1/2}$ ranges are for the 2+/1+ couples. [s] Reference 111. [t] This range is for only five of the isomers. [u] This range is for only four of the isomers.

(99) Yanilkin, V. V.; Gubskaya, V. P.; Morozov, V. I.; Nastapova, N. V.; Zverev, V. V.; Berdnikov, E. A.; Nuretdinov, I. A. *Russ. J. Electrochem.* **2003**, *39*, 1147−1165.
(100) Boudon, C.; Gisselbrecht, J. P.; Gross, M.; Herrmann, A.; Ruttimann, M.; Crassous, J.; Cardullo, F.; Echegoyen, L.; Diederich, F. *J. Am. Chem. Soc.* **1998**, *120*, 7860−7868.
(101) Keshavzarz-K, M.; Knight, B.; Haddon, R. C.; Wudl, F. *Tetrahedron* **1996**, *52*, 5149−5159.
(102) Ocafrain, M.; Herranz, M. A.; Marx, L.; Thilgen, C.; Diederich, F.; Echegoyen, L. *Chem. Eur. J.* **2003**, *9*, 4811−4819.
(103) Irngartinger, H.; Fettel, P. W.; Escher, T.; Tinnefeld, P.; Nord, S.; Sauer, M. *Eur. J. Org. Chem.* **2000**, 455−465.
(104) Avent, A. G.; Birkett, P. R.; Carano, M.; Darwish, A. D.; Kroto, H. W.; Lopez, J. O.; Paolucci, D.; Roffia, S.; Taylor, R.; Wachter, N.; Walton, D. R. M.; Zerbetto, F. *J. Chem. Soc., Perkin Trans. 2* **2001**, 140−145.
(105) Carano, M.; da Ros, T.; Fanti, M.; Kordatos, K.; Marcaccio, M.; Paolucci, D.; Prato, M.; Roffia, S.; Zerbetto, F. *J. Am. Chem. Soc.* **2003**, *125*, 7139−7144.
(106) Caron, C.; Subramanian, R.; D'Souza, F.; Kim, J.; Kutner, W.; Jones, M. T.; Kadish, K. *J. Am. Chem. Soc.* **1993**, *115*, 8505−8506.
(107) Echegoyen, L. E.; Djojo, F. D.; Hirsch, A.; Echegoyen, L. *J. Org. Chem.* **2000**, *65*, 4994−5000.
(108) Boulas, P.; D'Souza, F.; Henderson, C. C.; Cahill, P. A.; Jones, M. T.; Kadish, K. *J. Phys. Chem.* **1993**, *97*, 13435−13437.
(109) Azamar-Barrios, J. A.; Dennis, T. J. S.; Sadhukan, S.; Shinohara, H.; Scuseria, G. E.; Penicaud *J. Phys. Chem. A* **2001**, *105*, 4627−4632.
(110) Hall, M. H.; Shevlin, P.; Lu, H.; Gichuhi, A.; Shannon, C. *J. Org. Chem.* **2006**, *71*, 3357−3363.
(111) Paulouccci, F.; Marcaccio, M.; Roffia, S.; Orlandi, G.; Zerbetto, F.; Prato, M.; Maggini, M.; Scorrano, G. *J. Am. Chem. Soc.* **1995**, *117*, 6572−6580.
(112) Meier, M. S.; Poplawska, M.; Compton, A. L.; Shaw, J. P.; Selegue, J. P.; Guarr, T. F. *J. Am. Chem. Soc.* **1994**, *116*, 7044−7048.
(113) Kadish, K.; Gao, X.; Gorelik, O.; Van Caemelbecke, E.; Suenobu, T.; Fukuzumi, S. *J. Phys. Chem. A* **2000**, *104*, 2902−2907.
(114) Fan, L.; Li, Y.; Li, F.; Li, Y.; Zhu, D. *Chem. Phys. Lett.* **1998**, *294*, 443−446.
(115) Claves, D.; Giraudet, J.; Hamwi, A.; Benoit, R. *J. Phys. Chem. B* **2001**, *105*, 1739−1742.
(116) Illescas, B. M.; Martin, N. *J. Org. Chem.* **2000**, *65*, 5986−5995.
(117) Deng, F.; Wang, G.-W.; Zhang, T.-H.; Jiao, L.-J.; Chen, S. *Chem. Commun.* **2004**, 1118−1119.
(118) Zhou, J.; Rieker, A.; Grosser, T.; Skiebe, A.; Hirsch, A. *J. Chem. Soc., Perkin Trans.* **1997**, *2*, 1−5.
(119) Yang, Y.; Arias, F.; Echegoyen, L.; Chibante, L. P. F.; Flanagan, S.; Robertson, A.; Wilson, L. J. *J. Am. Chem. Soc.* **1995**, *117*, 7801−7804.

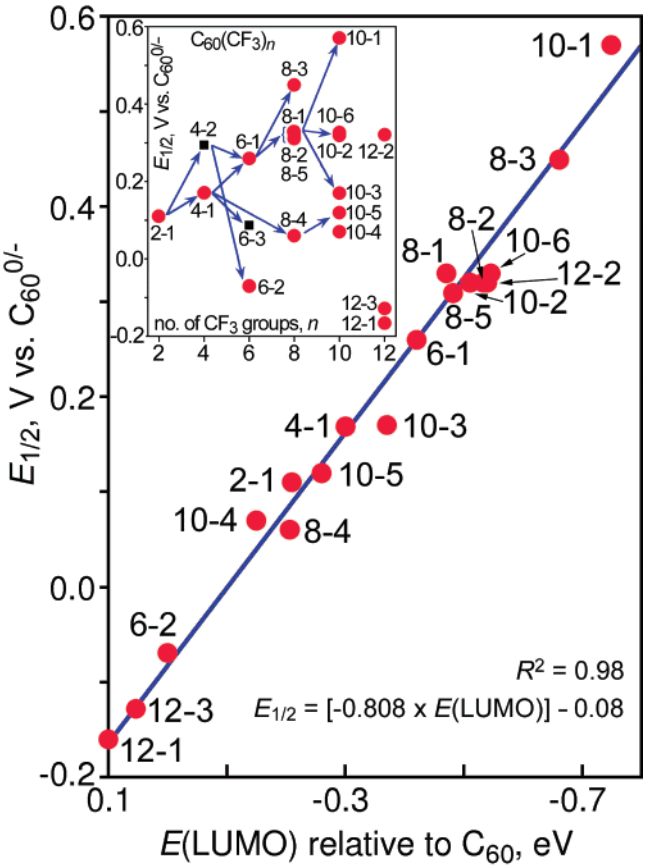

Figure 9. Plot of $E_{1/2}$ value for the $C_{60}(CF_3)_n^{0/-}$ couple (0.10 M $TBA^+BF_4^-$ in CH_2Cl_2; $E_{1/2}(C_{60}^{0/-}) = -0.98$ or -0.46 V vs $Fe(Cp)_2^{+/0}$ or $Fe(Cp^*)_2^{+/0}$ internal standards, respectively) vs the DFT-predicted LUMO energy. The linear least-squares fit to the data is shown at the bottom of the plot. The inset is a plot of the same $E_{1/2}$ values vs n, the number of CF_3 groups. The black squares represent $E_{1/2}$ values calculated using the least-squares equation in the main plot. Each arrow connects two compounds that are related by the addition of two (or four) CF_3 groups to specific positions. The arrows are intended to show structural relationships (cf. Schlegel diagrams in Figure 1) and not to imply that the mechanism of formation of the indicated compounds is by simple addition to two CF_3 groups to a fixed precursor (although this may, in the future, be shown to be true in some cases).

in Figure 9. (The p^3-$C_{60}(X)_4$ addition pattern of **4-2-CF$_3$** has been observed for X = 9-fluorenyl;[120] the as-yet unknown compound **4-2-CF$_3$** is predicted to be 8.2 kJ mol^{-1} more stable than **4-1**.[19]) The justification for including these hypothetical compounds in our analysis is the very good linear correlation of the experimental 0/− $E_{1/2}$ values with the PBE-predicted E(LUMO) values.

Note that **6-1** and **6-2**, which have 0/− $E_{1/2}$ values that differ by 0.33 V, can be envisioned as arising from the hypothetical common intermediate **4-2-CF$_3$** by adding two CF_3 groups to different pairs of cage carbon atoms (such comparisons are only meant to highlight structural relationships; nothing is implied here about the possible mechanism(s) by which **6-1** and **6-2** were formed). Similarly, **10-1**, **10-2**, and **10-3**, which have 0/− $E_{1/2}$ values of 0.57, 0.32, and 0.17 V vs $C_{60}^{0/-}$, respectively, can arise from **8-1** by adding two CF_3 groups to different pairs of cage carbon atoms. In fact, **10-1** and **10-3** differ in the placement of only one CF_3 group (see Figure 1), yet their reduction potentials differ by 0.40 V. Furthermore, the hypothetical transformation **8-1** + 2 CF_3 → **10-1** results in an increase in 0/− $E_{1/2}$, while the transformation **8-1** + 2 CF_3 → **10-3** results in a decrease in 0/− $E_{1/2}$.

Interestingly, the compound **6-2**, which has six electron-withdrawing CF_3 substituents, is harder to reduce than C_{60}, and **12-1** and **12-3**, with twice as many CF_3 groups as **6-2**, are 0.16 and 0.13 V harder to reduce than C_{60}, respectively. In contrast, the compound **12-2** is 0.32 V easier to reduce than C_{60}. It appears that the addition pattern is at least as important as, if not more important than, the value of n in determining the electron-acceptor properties of a particular $C_{60}(X)_n$ compound.

There are more isomers of $C_{60}(CF_3)_{12}$ than the three that have been characterized to date (i.e., **12-1**, **12-2**, and **12-3**),[28] and the same may be true for $C_{60}(CF_3)_{16}$ and $C_{60}(CF_3)_{18}$.[32] Nevertheless, none of the calculated 0/− $E_{1/2}$ values listed in Table 4 for isomers with n = 16 and 18 is more positive than the 0/− $E_{1/2}$ value of **10-1** or even **8-3**. It may be that saturation of the fullerene π system for $C_{60}(CF_3)_n$ derivatives with $n > 10$ places a limitation on how positive the 0/− $E_{1/2}$ value can be. Alternatively, with more than 12 CF_3 groups, addition-pattern fragments that lead to low LUMO energies may be uncommon. This issue will be considered after a discussion of substituent effects.

III. Correlation of LUMO Energies with Substituent Electronic Properties. Figure 6 shows the E(LUMO) values for 50 $C_{60}(X)_n$ compounds, and Figure S-14 shows the E(LUMO) values for 29 others. Except for the X = CF_3 derivatives and for $C_{60}(CH_3)_6$ with the **6-2** addition pattern,[64] the remaining compounds are hypothetical derivatives. The main significance of these results is not that they can be used to estimate $E_{1/2}$ values for nonexistent fullerene derivatives, it is because the observed trends led us to perform additional calculations and to discover a potentially general rule about the electron acceptor properties of exohedral fullerene derivatives.

The remaining π system in a fullerene$(X)_n$ compound is insulated from the electronic effects of the substituents by an sp^3 cage carbon atom. Therefore, for a given addition pattern, the LUMO energy should depend on the σ electron-donating or electron-withdrawing property of X (as well as on the cumulative saturation of the fullerene π system, which is probably independent of the nature of X). Even though the electronegativity of the cyano group is lower than those of the nitro group and a fluorine atom,[60] cyano groups attached to sp^3 cage carbon atoms[121] or methano carbon atoms[101] are known to produce strong anodic shifts in the first reduction relative to C_{60}. It was concluded that "the cyano substituent appears to be more electron-withdrawing than predicted by the Hammett [σ_m] relation."[101] The methyl derivatives have the least negative E(LUMO) values among the ten substituents studied for the eight addition patterns shown in Figures 6 and S-14, and the cyano derivatives have, with one minor exception, the most negative E(LUMO) values (the only exception is the **6-2** addition pattern, for which the **6-2-NO$_2$** E(LUMO) value is 0.032 eV more negative than the **6-2-CN** E(LUMO) value).

It is immediately apparent from the addition-pattern plots in Figure 6 that the *difference* between E(LUMO($C_{60}(CH_3)_n$)) and E(LUMO($C_{60}(CN)_n$)) increases as n increases from 2 to 10. This

(120) Murata, Y.; Shiro, M.; Komatsu, K. *J. Am. Chem. Soc.* **1997**, *119*, 8117−8118.

(121) Keshavzarz-K, M.; Knight, B.; Srdanov, G.; Wudl, F. *J. Am. Chem. Soc.* **1995**, *117*, 11371−11372.

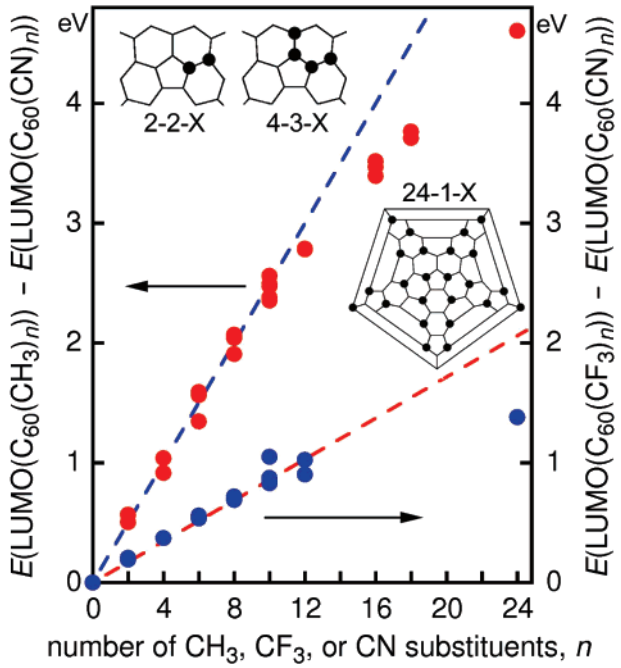

Figure 10. Plots of differences in E(LUMO) for pairs of $C_{60}(CH_3)_n$ and $C_{60}(CN)_n$ compounds with identical addition patterns (red circles) and for pairs of $C_{60}(CF_3)_n$ and $C_{60}(CN)_n$ compounds with identical addition patterns (blue circles) versus n, the number of substituents. There are two red and blue points for $n = 2$ and 12, three red and blue points for $n = 4$, four red and blue points for $n = 6$, five red and blue points for $n = 8$ and 10 (the compound **10-6** was omitted), two red and blue points for $n = 12$ (**12-3** was omitted), and one point for $n = 24$. The Schlegel diagram for T_h-$C_{60}(X)_{24}$ (with the **24-1-Br** addition pattern) and partial Schlegel diagrams for 1,9-$C_{60}(X)_2$ and 1,2,9,12-$C_{60}(X)_4$ (the **2-2-CN** and **4-3-F** addition patterns, respectively) are shown as insets.

is a sensible result: more substituents have a larger effect on the electronic structure of the fullerene derivative. It is also apparent that the increase in E(LUMO) from $C_{60}(CH_3)_n$ to $C_{60}(CH_3)_{n+2}$ *for these particular addition patterns* is nearly constant for $n = 2$, 4, 6, and 8 (0.23 ± 0.03 eV) *and* is equal in magnitude to the nearly constant decrease in E(LUMO) from $C_{60}(CN)_n$ to $C_{60}(CN)_{n+2}$ (0.24 ± 0.03 eV) for the same addition patterns. However, this was not found to be generally true: the difference between the E(LUMO) values for **6-2-CH$_3$** and **10-2-CH$_3$**, which is 0.29 eV, is much smaller than the corresponding difference for **6-2-CN** and **10-2-CN**, which is 0.84 eV.

By far the most intriguing result of our DFT E(LUMO) investigation was that the difference between E(LUMO($C_{60}(CH_3)_n$)) and E(LUMO($C_{60}(CN)_n$)) was virtually the same for the **10-1** and **10-2** addition patterns (2.49 and 2.48 eV, respectively) and varied by only 0.24 eV for the **6-1** and **6-2** addition patterns (1.59 and 1.35 eV, respectively). We subsequently calculated E(LUMO($C_{60}(CH_3)_n$)) and E(LUMO($C_{60}(CN)_n$)) values for all of the addition patterns listed in Table 1 as well as for two addition patterns that have two or four CH_3 and CN substituents on contiguous cage carbon atoms (these addition patterns are known for $C_{60}H_2$, $C_{60}F_2$, $C_{60}(CN)_2$, $C_{60}(Bn)_2$, and $C_{60}H_4$ and $C_{60}F_4$). The upper plot in Figure 10 (which includes Schlegel diagrams for the **2-2-CN**,[121] **4-3-F**,[122] and **24-1-Br**[65,123] addition patterns) shows that the difference between E(LUMO($C_{60}(CH_3)_n$)) and E(LUMO($C_{60}(CN)_n$)) is remarkably constant for all addition patterns (i.e., all isomers) with a given value of n. For example, the difference [E(LUMO($C_{60}(CH_3)_n$)) $-$ E(LUMO($C_{60}(CN)_n$))] is 1.47 ± 0.12 eV for the four $n = 6$ isomers, 1.99 ± 0.08 eV for the five $n = 8$ isomers, 2.47 ± 0.09 eV for five $n = 10$ isomers (**10-6** was excluded), and 2.78 ± 0.01 eV for two $n = 12$ isomers (**12-3** was excluded).

The E(LUMO) differences between the X = CH_3 and X = CF_3 compounds (not shown) and between the X = CF_3 and X = CN compounds (also shown in Figure 10) have similarly small ranges for isomers with a given value of n, demonstrating that the upper plot in Figure 10, with regular, slightly decreasing, intervals between neighboring values of n up to $n = 24$, is not the accidental result of arbitrarily choosing X = CH_3 and CN as the σ-effect extremes; this appears to be a general rule for $C_{60}(X)_n$ derivatives, at least for the particular addition patterns we have investigated so far. Whether the rule is valid for all realistic addition patterns (i.e., those with at least one isolated example for any X substituent), whether there is a corresponding rule for isomers of cycloadducts with the same substituent and n value, and whether similar rules are found for exohedral derivatives of fullerenes other than C_{60} or for endohedral fullerenes remain to be seen.

The implications of the electrochemical and DFT results so far are that (i) the $E_{1/2}$ values are not a simple function of n but instead depend critically on the particular addition pattern (to the point where a $C_{60}(X)_n$ compound with a given X and n value can be either easier or harder to reduce than C_{60}, depending on its addition pattern) and (ii) the range of possible $E_{1/2}$ values for $C_{60}(X)_n$ compounds with an assortment of substituents X depends on the value of n in a uniform manner and is nearly independent of the addition pattern. For a given set of substituents, and to a good degree of approximation, one can imagine a one-dimensional $E_{1/2}$ scale with variable $\Delta E_{1/2}$ ranges that depend on n but not on the addition pattern, anchored at particular $E_{1/2}$ values that depend on the addition pattern but not on n.

IV. Correlation of LUMO Energies, Addition Patterns, and Double Bonds in Pentagons. The DFT code with the PBE functional used extensively in this study for geometry optimization significantly shortens the optimization time for molecules as large as $C_{60}(CF_3)_n$ relative to the more commonly used B3LYP functional. We have already shown that PBE-predicted E(LUMO) values correlate very well with $0/-$ $E_{1/2}$ values. Since so much of the discussion that follows depends on the interpretation of PBE-predicted cage C$-$C bond distances (for those compounds that have not had their structures determined by X-ray crystallography), further validation of the PBE functional is warranted. Figure S-17 shows plots of X-ray vs PBE-predicted cage C$-$C distances for **10-5** (this work), **10-2**,[26] and $C_{74}(CF_3)_{12}$.[124] The agreement is excellent; fewer than five of the 90 X-ray cage C$-$C distances for each compound deviate from the PBE-predicted distances by more than $\pm 3\sigma$. Figure S-17 also shows a plot of PBE- vs B3LYP-predicted cage C$-$C distances for $C_{74}(CF_3)_{12}$, none of which differs by more than 0.003 Å.[124] Furthermore, the conformations of the six pairs of symmetry-related CF_3 groups in the X-ray structure

(122) Boltalina, O. V.; Darwish, A. D.; Street, J. M.; Taylor, R.; Wei, X.-W. *Perkin Trans.* **2002**, *2*, 251−256.
(123) Tebbe, F. N.; Harlow, R. L.; Chase, D. B.; Thorn, D. L.; Campbell, G. C.; Calabrese, J. C.; Herron, N.; Young, R. J.; Wasserman, E. *Science* **1992**, *256*, 822−825.
(124) Shustova, N. B.; Popov, A. A.; Newell, B. S.; Miller, S. M.; Anderson, O. P.; Seppelt, K.; Bolskar, R. D.; Boltalina, O. V.; Strauss, S. H. *Angew. Chem., Int. Ed.* **2007**, *46*, 4111−4114.

of $C_{74}(CF_3)_{12}$, defined as F−C−C−C torsion angles, were matched by the PBE-predicted F−C−C−C torsion angles to within 1° for four pairs and to within 5° (54.4(1)° vs 51.5°) and 7° (47.1(1)° vs 54.0°) for the other two pairs. Finally, the shapes of the LUMOs or SOMOs discussed below (i.e., the relative cage-carbon atomic orbital contributions to these molecular orbitals) were plotted using the B3LYP functional instead of the PBE functional only because B3LYP gave unpaired spin densities that better matched the experimental ESR spectra of **4-1**$^-$ and **10-2**$^-$ (see Figure 7). (Recall that the LUMO and SOMO for a given compound are virtually indistinguishable (see Figure S-12 for three examples); we also observed that plots of the PBE- and B3LYP-predicted LUMOs were visually indistinguishable). In summary, one can be confident that the calculated cage C−C distances discussed below and cage-carbon atomic orbital contributions shown in the figures correspond very closely to the actual distances and unpaired spin densities on individual carbon atoms in $C_{60}(X)_n$ molecules and radical anions.

The 0/− $E_{1/2}$ potentials in Table 4 (or their corresponding *E*(LUMO) values) and the Schlegel diagrams in Figure 1 are correlated in ways that appear complicated at first but become sensible after closer inspection. Consider first the isomers with $n = 8$ and 10. These are 11 compounds with similar numbers of CF_3 groups, and hence a similar collective electron-withdrawing inductive effect, with first-reduction potentials that range from 0.06 to 0.57 V vs $C_{60}^{0/-}$. The 11 potentials can be divided into four ranges: 0.09 ± 0.03 V (**8-4**, **10-4**, and **10-5**); 0.17 V (**10-3**); 0.32 ± 0.01 V (**8-1**, **8-2**, **8-5**, **10-2**, and **10-6**); and ≥0.45 V (**8-3** and **10-1**). All seven compounds with potentials greater than 0.30 V have two conjugated *nt*-DBIPs. In every case, these *nt*-DBIPs are also in conjugation with a common hex−hex junction double bond, forming a fulvene-like fragment, *and for all seven compounds the fulvene fragment essentially defines the LUMO*, as shown for **6-1** (the LUMO is virtually identical to the SOMO for the **6-1**$^-$ radical anion), for **4-1** and **10-2** in Figure 7 (see also Figure S-18), and for **8-2**, **8-3**, **8-5**, and **10-1** in Figure 11. For **10-3**, the only isolated $C_{60}(CF_3)_n$ compound in which a fulvene fragment is isolated from the rest of the fullerene π system by six of the ten cage C(sp^3) atoms (see Figure 1), the potential is only 0.17 V. In this case, the LUMO is essentially a localized fulvene-like π^* molecular orbital (not shown), and this highly localized orbital leads to a relatively high *E*(LUMO) and a relatively low $E_{1/2}$ value for this molecule. In contrast, the isomers of $C_{60}(CF_3)_8$ and $C_{60}(CF_3)_{10}$ with $E_{1/2} > 0.30$ V all have fulvene fragments that are in conjugation with the rest of the fullerene π system and consequently have LUMOs that include, to varying extents, adjacent portions of the fullerene π system in addition to the large orbital contributions from the six fulvenoid carbon atoms (hereinafter referred to as delocalized fulvene-like LUMOs). In fact, even **6-1** ($E_{1/2} = 0.26$ V), with only six CF_3 groups but with a delocalized fulvene-like LUMO, has a higher 0/− $E_{1/2}$ value than **10-3**.

The compound **6-1** can be compared with one of its probable precursors, the hypothetical compound **4-2-CF$_3$**, which has a *para*−*para*−*para* ribbon of edge-sharing C_6X_2 hexagons and therefore has a fulvene fragment with an associated delocalized fulvene-like LUMO, as shown in Figure 11. In this case however, because the p^3 ribbon is not part of a longer ribbon

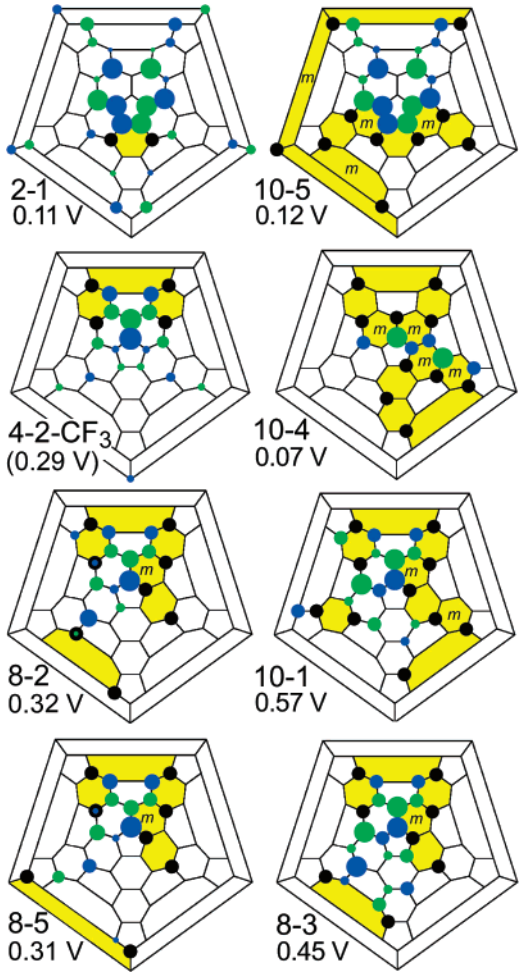

Figure 11. Schlegel diagrams showing the DFT-predicted cage carbon atom contributions to the LUMO of selected $C_{60}(CF_3)_n$ compounds. The blue (+) and green (−) circles represent the upper lobes of the π atomic orbitals for each cage carbon atom scaled approximately to its contribution to the LUMO. The $E_{1/2}$ values shown are for the $C_{60}(CF_3)_n^{0/-}$ couple vs the $C_{60}^{0/-}$ couple. The $E_{1/2}$ value for **4-2-CF$_3$** was calculated using the linear least-squares equation in Figure 9.

of edge-sharing C_6X_2 hexagons, as is the case with **6-1**, the LUMO of **4-2-CF$_3$** is more extensively delocalized on both sides of the fulvene fragment instead of only on one side as in the LUMO of **6-1**. It is probably for this reason that **4-2-CF$_3$**, with only four CF_3 groups, is predicted to have a 0/− $E_{1/2}$ value (0.29 V) which is slightly more positive than the $E_{1/2}$ value of **6-1**, with six CF_3 groups (0.26 V), as shown in Figure 9.

The second isolable isomer of $C_{60}(CF_3)_6$, **6-2**,[21] also has a pair of conjugated DBIPs, but in this case they each have only one C(sp^2) nearest neighbor, not two. In addition, this *cis*-butadiene fragment is isolated from the rest of the fullerene π system. As a consequence, the LUMO is not associated with this pair of short *t*-DBIPs (PBE-predicted distance = 1.358 Å[21]) but instead forms a localized LUMO antipodal to the skew-pentagonal-prism array of CF_3 groups, as shown in Figure S-12 (see SI). Furthermore, this orbital has considerably more antibonding character than does the delocalized fulvene-like LUMO of **6-1**. In addition, adding an electron to the LUMO of **6-1** shortens the long C−C bonds and lengthens the short bonds in the fulvene fragment, making this fragment slightly more aromatic than the neutral compound (see Figure S-18 in SI). The combination of these factors results in *E*(LUMO) values

for this pair of compounds that differ by 0.42 eV and $E_{1/2}$ values that differ by 0.33 V (with an anodic shift from C_{60} in the case of **6-1** and cathodic shift from C_{60} in the case of **6-2**). The compound **12-3**, with two isolated *cis*-butadiene LUMO fragments, is similar to **6-2** in its electrochemical behavior.

A compound with two isolated *cis*-butadiene fragments is **10-4**. Unlike **6-2**, however, **10-4** also has two *nt*-DBIPs, and they form a *trans*-butadiene-like fragment that is in conjugation with the main π system of the molecule (the experimental and PBE-predicted distances for the symmetry-related *nt*-DBIPs in **10-4** are 1.365(3) and 1.376 Å, respectively). The LUMO of **10-4**, shown in Figure S-10, resembles the LUMO of *trans*,*trans*,*trans*-octatetraene. This orbital has much more antibonding character and much less bonding character than do the LUMOs of the molecules with fulvene fragments. Consequently, it is clear why **10-4** has a first-reduction potential (0.07 V) that is cathodically shifted by 0.10 V from **10-3**, with its isolated fulvene LUMO, and cathodically shifted by 0.25 V or more from **10-1** and **10-2**, with their delocalized fulvene-like LUMOs. Nevertheless, in all cases discussed so far, molecules with two conjugated *nt*-DBIPs have LUMOs that include significant p-orbital contributions from these four cage C atoms.

So far, two factors that significantly affect the $E_{1/2}$ values of $C_{60}(CF_3)_n$ compounds (and probably those of other $C_{60}(X)_n$ compounds with similar structures) have been identified: (i) compounds with a p^3 ribbon fragment of edge-sharing C_6X_2 hexagons have LUMO fragments that resemble the LUMO of the hydrocarbon fulvene and have high $E_{1/2}$ values relative to those of isomers without a p^3 ribbon fragment; and (ii) the degree to which the LUMO is delocalized (i.e., conjugated to the rest of the fullerene π system) strongly affects the 0/− $E_{1/2}$ value (because it affects *E*(LUMO); this, of course, is a general principle of any molecular orbital formalism, including Hückel MO theory). The number of substituents is *not* among the most influential factors.

There are several compounds we have studied electrochemically that do not have two *nt*-DBIPs forming a fulvene fragment but instead have only one *nt*-DBIP. These are **2-1**, **4-1**, **8-4**, and **10-5**. The 0/− $E_{1/2}$ values for **2-1** (0.11 V vs $C_{60}^{0/-}$) and **10-5** (0.12 V) are the same to within experimental error, despite the large difference in the number of CF_3 substituents. As far as *E*(LUMO) and $E_{1/2}$ values are concerned, it appears that too many electron-withdrawing groups can be "too much of a good thing" in some cases. Close inspection of Figure 11 reveals that the LUMO for **2-1** is more delocalized, on the far side of the molecule (i.e., the side opposite the main part of the LUMO), than the **10-5** LUMO because **10-5** has multiple CF_3 groups on the far side and **2-1** does not.

The main part of the LUMO for **2-1**, **4-1**, **8-4**, and **10-5** resembles the LUMO of acenaphthalene. Adding an electron to the LUMO of acenaphthalene or **2-1** shortens the long C−C bonds and lengthens the short ones in acenaphthalene or the acenaphthalene fragment of **2-1**, making them slightly more aromatic (see Figure S-19 in SI), but to a lesser extent than was observed for fulvene or the fulvene fragment of **10-2**. Consequently, which kind of LUMO fragment leads to a higher first-reduction potential, fulvene or acenaphthalene? Our results clearly show that a fulvene-like LUMO for a $C_{60}(CF_3)_n$ derivative makes that derivative easier to reduce than an acenaphthalene-like LUMO when $n = 4$ (**4-2** vs **4-1**), when $n = 10$ (**10-2** vs **10-5**), and presumably for other n values, all other things being equal.

Nevertheless, an acenaphthalene-like LUMO appears to have a lower energy than LUMOs that arise from 1,2 additions. This was first pointed out by Kadish et al., who reported that **2-1-Bn** was 0.10 V easier to reduce than **2-2-Bn**[62] and that **4-1-Bn** was 0.05 V easier to reduce than another isomer of $C_{60}(Bn)_4$ with an *ortho-meta-para* addition pattern.[57] Wudl et al. found that the first-reduction potential of **2-2-CN** was 0.12 V vs $C_{60}^{0/-}$,[121] but the first-reduction potential of **2-1** is essentially the same relative to $C_{60}^{0/-}$, 0.11 V, even though the cyano group is a much better electron-withdrawing group than the trifluoromethyl group (see Figure 6). Furthermore, the PBE-predicted first-reduction potential for **2-2-CF$_3$** is 0.03 V, 80 mV lower than the measured value for **2-1** (and 60 mV lower than the predicted value for **2-1**). Another example is the 0.140 eV difference in *E*(LUMO) values for **4-1-F** and **4-3-F**, which are −4.761 eV and −4.621 eV, respectively.

Now we can return to the seven isomers of $C_{60}(CF_3)_8$ and $C_{60}(CF_3)_{10}$ with $E_{1/2} \geq 0.30$ V. These are **8-1**, **8-2**, **8-5**, **10-2**, and **10-6** with $E_{1/2} = 0.32 \pm 0.01$ V, and **8-3** and **10-1**, with $E_{1/2} \geq 0.45$ V. All have a fulvene fragment with two *nt*-DBIPs. Why are **8-1** and **8-3** separated by 0.12 V? Why are **10-2** and **10-1** separated by 0.25 V? The simple, but incomplete, answer is that **8-1** and **10-2** *only* have the fulvene fragment *nt*-DBIPs but **8-3** and **10-1** also have another *nt*-DBIP (the one that is associated with the isolated *p*-$C_6(CF_3)_2$ hexagon in the **8-3** and **10-1** addition patterns), and this provides **8-3** and **10-1** with LUMOs that have fulvene-like and acenaphthalene-like fragments that overlap. These extensively delocalized LUMOs lead to the highest 0/− $E_{1/2}$ values for all $C_{60}(CF_3)_n$ compounds with $n = 2-18$ listed in Table 4. The reason this answer is incomplete is because **8-2**, **8-5**, and **10-6**, as does **8-3**, have an additional *nt*-DBIP associated with their isolated *p*-$C_6(CF_3)_2$ hexagons, or, in the case of **10-6**, its *pmp* fragment.

Why then are the $E_{1/2}$ values for **8-2**, **8-5**, and **10-6** 0.13 ± 0.01 V lower than for **8-3**? The answer to that question is as follows. The position of some isolated *p*-$C_6(CF_3)_2$ hexagons, like those in **8-3** and **10-1**, allows the acenaphthalene-like π^* fragment associated with the *nt*-DBIP to overlap with the fulvene-like π^* fragment associated with the conjugated pair of *nt*-DBIPs, and when that occurs, the LUMO of the molecule includes both π^* fragments, is extensively delocalized, and has a relatively low energy (see Figure 11). For **8-2**, **8-5**, and **10-6**, on the other hand, the two π^* fragments are farther apart and do not overlap (i.e., the two fragments do not contain cage carbon atoms in common). In these cases, the LUMO is essentially a delocalized fulvene-like π^* orbital very similar to the LUMO of **8-1**, and all three molecules have the same first-reduction potential to within experimental error. Interestingly, the LUMO+1 orbitals of **8-2**, **8-5**, and **10-6** are essentially an acenaphthalene-like π^* orbital, much like the LUMOs of **2-1** and **4-1**. In fact, the LUMO+1 energies of **8-2** and **8-5** (−4.594 and −4.666 eV, respectively) are the same to within 0.016 eV as the LUMO energies of **2-1** and **4-1** (−4.592 and −4.682 eV, respectively).

The recently reported compound **12-2**[28] has the same situation as **8-2**, **8-5**, and **10-6**: the three *nt*-DBIPs give rise to a fulvene-like LUMO and an acenaphthalene-like LUMO+1 instead of combining to form one lower-energy LUMO, and consequently,

the first-reduction potential of **12-2** is same as the $E_{1/2}$ for **8-2**. The separation of the **12-2** fulvene-like π* fragment and the acenaphthalene-like π* fragment into two separate empty orbitals is clearly shown in Figure S-20 (see SI). This lower energy of the fulvene-like LUMO relative to that of the acenaphthalene-like LUMO+1 reinforces the conclusion stated earlier that, if the goal is to prepare a better one-electron acceptor fullerene derivative, addition patterns that produce fulvene-like π* fragments are more desirable than those that produce acenaphthalene-like π* fragments.

It is ironic that double bonds in pentagons, which are destabilizing as far as the total energy of a fullerene derivative is concerned,[52,53] are exactly what is needed to lower the energy of its LUMO and increase its electron affinity. However, DBIPs are necessary but not sufficient. Most $C_{60}(CF_3)_n$ compounds have numerous *t*-DBIPs (i.e., the blue DBIPs in Figure S-8), and these are among the shortest C−C bonds in the cage (see the X-ray structures cited in Table 1). None of the LUMOs we have examined are ever associated with *t*-DBIPs. Only *nt*-DBIPs with two C(sp^2) nearest neighbors generate low-energy π* fragments that are incorporated into the LUMO. The compound **12-1**, for example, has six *t*-DBIPs and twelve electron-withdrawing CF_3 groups but is 0.16 V more difficult to reduce than C_{60} (this addition pattern was previously predicted by Dixon et al.[53] to lead to high *E*(LUMO) values relative to C_{60}, even for $C_{60}F_{12}$).

We have predicted the 0/− $E_{1/2}$ values for the recently reported compounds **16-1**, **16-2**, **16-3**, **18-1** and for the hypothetical compound **18-2**, and they are listed in Table 4. The LUMOs for four of these compounds have one or more fulvene-like π* fragments, none of which overlap with each other; the LUMO for **16-2** does not resemble any obvious aromatic hydrocarbon fragment (all five LUMOs are shown as Schlegel diagrams in Figure S-21). None of these compounds is predicted to be easier to reduce than **8-3**. The compound **16-1** has an $E_{1/2}$ value of only 0.04 V vs $C_{60}^{0/-}$. The highest predicted $E_{1/2}$ value for these five compounds is for **18-2** (0.36 V vs $C_{60}^{0/-}$), which has a LUMO with three isolated fulvene π* fragments.

The concept that the overlap of two π* fragments can combine to produce a low-energy LUMO led to the search for an addition pattern with a higher $E_{1/2}$ value than **10-1**. The C_2-symmetry compound **8-7-CF$_3$**, which has two separate p^3 ribbons of edge-sharing *p*-$C_6(CF_3)_2$ hexagons, as shown in Figure S-22, has a LUMO in which the two fulvene-like π* fragments are efficiently overlapped and has predicted *E*(LUMO) and 0/− $E_{1/2}$ values that are 1.000 eV lower and 0.73 V higher, respectively, than that of C_{60}. This hypothetical isomer of $C_{60}(CF_3)_8$ is only 13 kJ higher in energy than **8-2**, the most stable isomer of this composition (see Table S-2 in SI).

In summary, for the numerous addition patterns we have investigated, the electronic properties of substituents as diverse as CH_3 and CN can produce variations in $C_{60}(X)_n$ $E_{1/2}$ values of more than 3 V. The variation depends on the value of *n* but is almost independent of the addition pattern. For a given substituent, the range of experimentally observed $E_{1/2}$ values depends on *n*, but the range for a set of isomers can be so large (e.g., up to 0.5 V for $n = 10$) that it is essentially the addition pattern, not the value of *n*, that determines the particular $E_{1/2}$ value for a given compound. From the standpoint of designing better electron acceptors, structures with *nt*-DBIPs are essential, and therefore 1,4 additions are better than 1,2 additions. Furthermore, (i) addition patterns that produce a delocalized fulvene-like π* fragment are better than those that produce an acenaphthalene-like π* fragment, (ii) addition patterns that result in the overlap of fulvene-like and acenaphthalene-like π* fragments are even better yet, and (iii) addition patterns that result in the overlap of two fulvene-like π* fragments are best.

V. Correlations Involving −/2− and 2−/3− $E_{1/2}$ Values. Sixteen second reductions and ten third reductions were reversible (as defined earlier). Although the second added electron should, in principle, be paired with the first added electron in the LUMO (unlike C_{60}, which has a triply degenerate LUMO, all 16 $C_{60}(CF_3)_n$ compounds with a reversible second reduction have C_s, C_2, C_{2h}, or C_1 symmetry and therefore cannot have degenerate orbitals), there was a poor correlation between the *E*(LUMO) and −/2− $E_{1/2}$ values. There was also a poor correlation between the *E*(LUMO+1) and 2−/3− $E_{1/2}$ values. Since the poor correlations might be due to (i) the increasing solvation energies of the $C_{60}(CF_3)_n^{m-}$ anions as *m* increases and (ii) structural and electronic reorganization following electron transfer, we decided to compute the energies of the $C_{60}(CF_3)_n^{m-}$ and $C_{60}(CF_3)_n^{(m+1)-}$ anions in the gas phase as well as their solvation free energies in dichloromethane and to model the reduction potential as the difference in energy between the solvated $C_{60}(CF_3)_n^{m-}$ and $C_{60}(CF_3)_n^{(m+1)-}$ anions.

The electrostatic contribution to the solvation free energies were calculated using the Born model (BM) and the conductor-like polarizable model (C-PCM; see Experimental Section). The effective radius of each ion used for the BM calculations was the cube root of 75% of the C-PCM cavity volume. The computed solvation energies, which decreased as *n* increased (because of the increase in volume as *n* increased), were similar for both models. The C-PCM results are listed in Table S-3 along with the B3LYP-predicted electron affinities and reduction potentials. (The B3LYP-predicted *EA*(1) values for C_{60} and C_{70}, 2.519 and 2.594 eV, respectively, are only ca. 0.15 eV lower than the experimental values, 2.666(1) eV)[4,5] and 2.676(1) eV,[4] respectively.) Note that the electrostatic solvation energies of the neutral compounds are all less than 0.1 eV.

As expected, the predicted *EA*(1) values for $C_{60}(CF_3)_n$ derivatives are higher than for C_{60}. The values for **4-1** (2.961 eV), **6-1** (3.145 eV), the five isomers of $C_{60}(CF_3)_8$ (2.961−3.448 eV), and the five isomers of $C_{60}(CF_3)_{10}$ (3.010−3.612 eV), compare favorably with the experimental *EA*(1) values for samples of $C_{60}(CF_3)_{4-10}$ consisting of an unknown mixture of isomers, which are 3.03 ± 0.20 eV[125] and 3.17 ± 0.19[126] for $C_{60}(CF_3)_4$, 3.04 ± 0.14[125] and 3.17 ± 0.16 eV[126] for $C_{60}(CF_3)_6$, 3.07 ± 0.06[125] and 3.12 ± 0.18 eV[126] for $C_{60}(CF_3)_8$, and 3.200 or 3.245 eV for $C_{60}(CF_3)_{10}$.[125] However, the experimental values are virtually the same to within the quoted errors, but our calculations show that the ranges of *EA*(1) values for a set of isomers can be as large as 0.6 eV.

The B3LYP-predicted *EA*(2) values for some of the $C_{60}(CF_3)_n$ compounds are positive, which indicates that their dianions should be stable species in the gas phase. Indeed, $C_{60}(CF_3)_n^{2-}$

(125) Markov, V. Y.; Aleshina, V. E.; Borschevskii, A. Y.; Khatymov, R. V.; Tuktarov, R. F.; Pogulay, A. V.; Maximov, A. L.; Kardashev, S. V.; Ioffe, I. N.; Avdoshenko, S. M.; Dorozhkin, E. I.; Goryunkov, A. A.; Ignat'eva, D. V.; Gruzinskaya, N. I.; Sidorov, L. N. *Int. J. Mass Spectrom.* **2006**, *251*, 16−22.

(126) Borschevskii, A. Y.; Aleshina, V. E.; Markov, V. Y.; Dorozhkin, E. I.; Sidorov, L. N. *Inorg. Mater.* **2005**, *41*, 1318−1326.

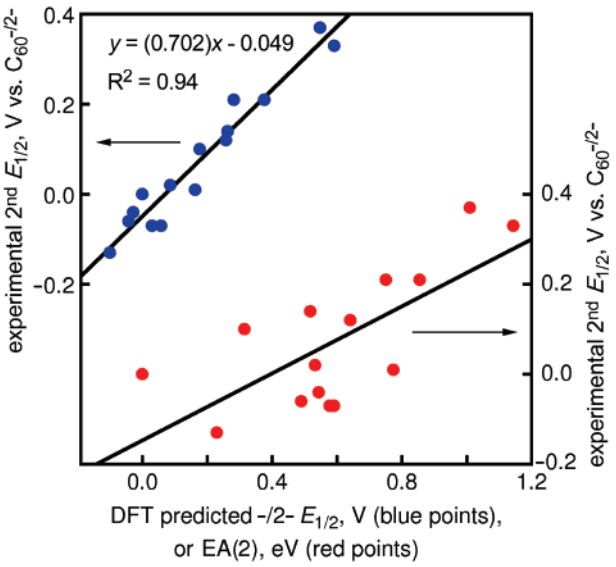

Figure 12. Plots of experimental second-reduction potentials of 18 $C_{60}(CF_3)_n$ compounds (relative to the $C_{60}^{-/2-}$ potential) vs the B3LYP-predicted relative second reduction potentials relative to the predicted $C_{60}^{-/2-}$ potential (blue points) or the B3LYP-predicted second gas-phase electron affinities relative to the predicted *EA*(2) for C_{60} (red points).

($n = 2-20$) dianions were generated recently by collisions of the corresponding monoanions produced in an electrospray ion source with sodium atoms.[127] Cross sections for electron capture by monoanions decreased on going from $n = 10$ to $n = 20$. Figure 12 displays plots of 17 experimental $-/2-$ $E_{1/2}$ values (including $C_{60}^{-/2-}$) vs (i) B3LYP-predicted *EA*(2) values (relative to C_{60}) and (ii) B3LYP-predicted $-/2-$ $E_{1/2}$ values (i.e., the difference in ΔG_{solv} of $C_{60}(CF_3)_n^{(m+1)-}$ and $C_{60}(CF_3)_n^{m-}$ minus the *EA*(m+1) value, also relative to C_{60}). The correlation between the experimental $E_{1/2}$ values and *EA*(2) is poor ($R^2 = 0.50$), but when corrected for the differences in ΔG_{solv} for the mono- and dianions, the correlation is sufficiently better ($R^2 = 0.94$) so that $-/2-$ $E_{1/2}$ values predicted for $C_{60}(CF_3)_n$ compounds not yet examined by cyclic voltammetry are probably reliable to ±0.04 V. Note that there are no points for **8-5** and **12-1** in Figure 12 because these compounds do not have reversible second reductions.

As expected, solvation corrections also improved the correlation between experimental $0/-$ $E_{1/2}$ values and B3LYP-predicted *EA*(1) values (not shown). However, even when solvation was taken into account, the B3LYP-predicted third-reduction potentials were poorly correlated with the experimental values. This may be because the electrostatic contributions to the solvation energies for the $C_{60}(CF_3)_n^{3-}$ trianions are very large (ca. 8−10 eV), and relatively small uncertainties in anion volumes lead to larger errors in $E_{1/2}$ values for the third reductions than for the first and second reductions.

The connection between addition pattern and *E*(LUMO) discussed in the previous section should prove useful in understanding gas-phase electron affinities (*EA*s) as well as solution $E_{1/2}$ values. In addition to their fundamental importance, reliable electron affinities of fullerene(X)$_n$ compounds, whether determined experimentally or predicted with a validated computational method, can be used to estimate negative ion chemical- or electrospray-ionization sensitivities, which can be useful for the compositional analysis of reaction mixtures by mass spectrometry.[128]

Summary and Conclusions

Experimental reduction potentials for 18 $C_{60}(CF_3)_n$ compounds have demonstrated that the addition pattern is as important, if not more important in many cases, than the number of substituents, n, in determining $E_{1/2}$ values. DFT calculations demonstrate that those addition patterns with double bonds in pentagons having two C(sp^2) neighbors result in the strongest electron acceptors. Specifically, (i) compounds with a delocalized fulvene-like π^* fragment are better electron acceptors than those with an acenaphthalene-like π^* fragment, (ii) compounds with addition patterns that result in the overlap of fulvene-like and acenaphthalene-like π^* fragments are better yet, and (iii) compounds with addition patterns that result in the overlap of two fulvene-like π^* fragments are predicted to be the best electron acceptors.

Acknowledgment. We dedicate this paper to Neil Bartlett on the occasion of his 75th birthday. He has always been and continues to be both a friend and an inspiration to us and many others in the field of fluorine chemistry. We appreciate the financial support of the DAAD, the Volkswagen Foundation (I-77/855), the Fonds der Chemischen Industrie, Germany, the Russian Foundation for Basic Research (06-03-33147-a), the Russian Federal Agency of Science and Innovations (Contract 02.442.11.7439), the Civilian Research and Development Foundation (RUC2-2830-MO-06), the U.S. National Science Foundation (CHE-0707223 and, for partial support of EBS, CHE-0416017), and the Colorado State University Research Foundation. We thank Karl F. Freed for encouragement and assistance, Manfred Kappes for generous support, Donald L. Dick for assistance with APCI mass spectrometry, Xiang Gao for digitized absorption spectra of the two isomers of $C_{60}(Bn)_4$, and Karl Kadish, Carlo Thilgen, and Warren Powell for helpful discussions.

Supporting Information Available: Crystallographic data in CIF format, complete references 40 and 73, and additional figures and tables. This material is available free of charge via the Internet at http://pubs.acs.org.

JA073181E

(127) Streletskiy, A. V.; Hvelplund, P.; Nielsen, S. B.; Liu, B.; Tomita, A.; Goryunkov, A. A.; Boltalina, O. V. *J. Chem. Phys.* **2006**, *124*, 144306−144316.
(128) Betowski, L. D.; Enlow, M.; Aue, D. H. *Int. J. Mass Spectrom.* **2006**, *255*−*256*, 123−129.